



# Feedback Between Carbon and Nitrogen Cycles During the Ediacaran Shuram Excursion

Dongtao Xu<sup>1</sup>, Xinqiang Wang<sup>1,2\*</sup>, Xiaoying Shi<sup>1,2</sup>, Yongbo Peng<sup>3,4</sup> and Eva E. Stüeken<sup>5</sup>

<sup>1</sup>School of Earth Science and Resources, China University of Geosciences (Beijing), Beijing, China, <sup>2</sup>State Key Laboratory of Biogeology and Environmental Geology, China University of Geosciences (Beijing), Beijing, China, <sup>3</sup>International Center for Isotope Effect Research, Nanjing University, Nanjing, China, <sup>4</sup>School of Earth Sciences and Engineering, Nanjing University, Nanjing, China, <sup>5</sup>School of Earth and Environmental Sciences, University of St Andrews, St Andrews, United Kingdom

## OPEN ACCESS

### Edited by:

Jon Telling,  
Newcastle University, United Kingdom

### Reviewed by:

Qing Li,  
Qingdao Institute of Marine Geology  
(QIMG), China  
Christophe Thomazo,  
Université de Bourgogne, France

### \*Correspondence:

Xinqiang Wang  
wxqiang307@126.com

### Specialty section:

This article was submitted to  
Geochemistry,  
a section of the journal  
Frontiers in Earth Science

**Received:** 09 March 2021

**Accepted:** 11 May 2021

**Published:** 25 May 2021

### Citation:

Xu D, Wang X, Shi X, Peng Y and  
Stüeken EE (2021) Feedback Between  
Carbon and Nitrogen Cycles During  
the Ediacaran Shuram Excursion.  
*Front. Earth Sci.* 9:678149.  
doi: 10.3389/feart.2021.678149

The middle Ediacaran Period records one of the deepest negative carbonate carbon isotope ( $\delta^{13}\text{C}_{\text{carb}}$ ) excursions in Earth history (termed the Shuram excursion). This excursion is argued by many to represent a large perturbation of the global carbon cycle. If true, this event may also have induced significant changes in the nitrogen cycle, because carbon and nitrogen are intimately coupled in the global ocean. However, the response of the nitrogen cycle to the Shuram excursion remains ambiguous. Here, we reported high resolution bulk nitrogen isotope ( $\delta^{15}\text{N}$ ) and organic carbon isotope ( $\delta^{13}\text{C}_{\text{org}}$ ) data from the upper Doushantuo Formation in two well-preserved sections (Jiulongwan and Xiangerwan) in South China. The Shuram-equivalent excursion is well developed in both localities, and our results show a synchronous decrease in  $\delta^{15}\text{N}$  across the event. This observation is further supported by bootstrapping simulations taking into account all published  $\delta^{15}\text{N}$  data from the Doushantuo Formation. Isotopic mass balance calculations suggest that the decrease in  $\delta^{15}\text{N}$  during the Shuram excursion is best explained by the reduction of isotopic fractionation associated with water column denitrification ( $\epsilon_{\text{wd}}$ ) in response to feedbacks between carbon and nitrogen cycling, which were modulated by changes in primary productivity and recycled nutrient elements through remineralization of organic matter. The study presented here thus offers a new perspective for coupled variations in carbon and nitrogen cycles and sheds new light on this critical time in Earth history.

**Keywords:** Ediacaran, South China, Doushantuo Formation, Shuram excursion, nitrogen isotopes

## INTRODUCTION

Unraveling the global carbon cycle in deep time of Earth history mostly relies on the analyses of carbon isotope compositions in carbonate rocks ( $\delta^{13}\text{C}_{\text{carb}}$ ) and organic matter ( $\delta^{13}\text{C}_{\text{org}}$ ) (Kump and Arthur, 1999). With the expansion of  $\delta^{13}\text{C}_{\text{carb}}$  datasets over the past 2 decades (cf. Lyons et al., 2014), a general  $\delta^{13}\text{C}_{\text{carb}}$  picture from the Archean to present has become evident. A major feature of this curve is that the magnitude of isotopic variation in the Precambrian is much larger than that of the Phanerozoic, as exemplified by the notable Shuram negative  $\delta^{13}\text{C}_{\text{carb}}$  excursion documented in the middle Ediacaran (Burns and Matter, 1993; Fike et al., 2006; Le Guerroué et al., 2006a, 2006b). This excursion and its possible equivalents are widely distributed in Ediacaran successions all over the world and have been generally used as a tie-point for the stratigraphic correlations across different

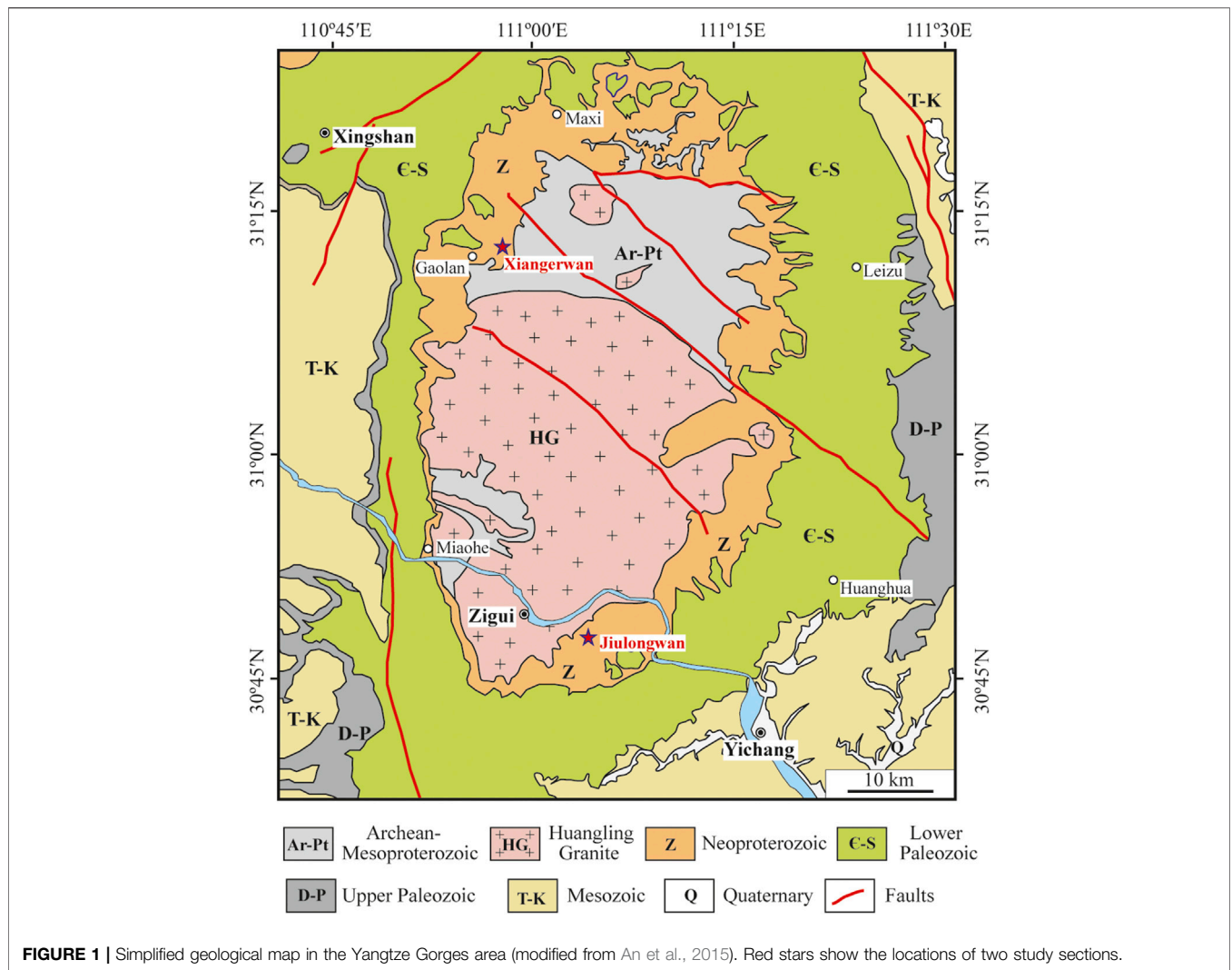
continents (Jiang et al., 2007; Zhu et al., 2007; Halverson et al., 2010; Grotzinger et al., 2011; Wang et al., 2012; Lu et al., 2013; Husson et al., 2015; Wang et al., 2016; Zhou et al., 2017), although whether they are truly synchronous remains to be tested independently by precise radiometric ages (Grotzinger et al., 2011; Zhou et al., 2017).

Among all negative  $\delta^{13}\text{C}_{\text{carb}}$  excursions from the Archean to Phanerozoic, the Shuram excursion is remarkable for two reasons: first, it is one of the largest negative excursions in Earth history, with  $\delta^{13}\text{C}_{\text{carb}}$  decreasing from +5‰ to as low as -12‰ (Grotzinger et al., 2011); second, it may have lasted for millions of years (~5–50 Myr) before returning to positive values (Le Guerroué et al., 2006a, 2006b; Bowring et al., 2007; Jiang et al., 2007; Cui et al., 2015; Sui et al., 2019; Canfield et al., 2020; Gong and Li, 2020; Rooney et al., 2020). The anomalously low  $\delta^{13}\text{C}_{\text{carb}}$  values (down to -12‰) during the Shuram excursion are below the mantle-derived carbon isotope value of -6‰ (Melezhik et al., 2005) and can therefore not be readily explained by the conventional steady-state mass balance model of carbon isotopes (Kump and Arthur, 1999). Several non-steady-state models link the Shuram excursion to the rise of oxygen in the atmosphere-ocean system, which may have resulted in the oxidation of an inferred large dissolved organic carbon (DOC) reservoir in deep ocean (Rothman et al., 2003; Fike et al., 2006; Jiang et al., 2007; McFadden et al., 2008) and/or other reduced carbon sources, including terrestrial organic matter (Kaufman et al., 2007; Shi et al., 2018), methane hydrates (Bjerrum and Canfield, 2011) and expelled hydrocarbons (Lee et al., 2015). These models imply that the Shuram excursion recorded the primary isotopic composition of seawater, which is further supported by a recent *in situ* carbon isotope study from the Wonoka Formation in Australia (Husson et al., 2020). These hypotheses have been challenged on the basis that the oxidant budget may have been insufficient if the Shuram excursion lasted for more than 5 Myr (Bristow and Kennedy, 2008); however, recent biogeochemical modeling results suggest that the oxidants required for the oxidation of DOC could have derived from the weathering of sulfate evaporites (Shields et al., 2019). Alternatively, the Shuram excursion has been interpreted as reflecting secondary processes such as meteoric alteration (Knauth and Kennedy, 2009; Swart and Kennedy, 2012), burial diagenesis (Derry, 2010), or the contribution from authigenic carbonates (Schrage et al., 2013; Cui et al., 2017; Jiang et al., 2019). However, these diagenetic processes, which are essentially local phenomena, are difficult to reconcile with the global distribution of the Shuram excursion and its unique occurrence in the Ediacaran (Grotzinger et al., 2011). Additionally, Paulsen et al. (2017) argued that the Shuram excursion may be partially attributed to extensive release of mantle  $^{12}\text{C}$ -enriched carbon associated with carbonatite and alkaline magmatism during the Ediacaran period, but the extremely low  $\delta^{13}\text{C}_{\text{carb}}$  values of the Shuram excursion still require additional input from surface processes.

The carbon cycle has intimate relationships with the nitrogen and oxygen cycles in the global ocean (Fennel et al., 2005). Nitrogen is one of the major nutrient elements required for all life. In the excess of bioavailable P, fixed N may

become an important limiting nutrient in the ocean and thereby control the amount of carbon sequestered into sediments and the rate of oxygen production through photosynthesis (Falkowski, 1997; Tyrrell, 1999). Conversely, the concentration of fixed N is mainly determined by the balance between  $\text{N}_2$  fixation, the major pathway of N into aquatic ecosystems, and the reconversion of fixed nitrogen to  $\text{N}_2$  gas mainly via denitrification (stepwise reduction of nitrate to  $\text{N}_2$ ) and anammox (coupled oxidation of ammonium with reduction of nitrite) (Sigman et al., 2009; Devol, 2015), which in turn is largely dependent on the ocean redox structure (Quan et al., 2013; Ader et al., 2016; Stüeken et al., 2016). During denitrification, organic matter is an important electron donor (Sigman et al., 2009), although it can be replaced by ferrous Fe(II) or hydrogen sulfide ( $\text{H}_2\text{S}$ ) (Lam and Kuypers, 2011; Michiels et al., 2017). Coupled nitrate ( $\text{NO}_3^-$ ) reduction and the oxidation of organic matter through denitrification would result in the transformation of  $^{12}\text{C}$ -enriched organic carbon to inorganic carbon, and the preferential release of light  $^{14}\text{N}$  to the atmosphere, thereby elevating the  $\delta^{15}\text{N}$  in the fixed N pool and lowering the  $\delta^{13}\text{C}$  of the dissolved inorganic carbon pool (Sigman et al., 2009; Kump et al., 2011). Further, the remineralization of organic matter in the oceans would release the organic-bound N into seawater with limited nitrogen isotopic fractionation (-1 to +2‰, Ader et al., 2016; Stüeken et al., 2016), which could serve as new nutrient N source to fuel productivity (Higgins et al., 2012; Xu et al., 2020).

The Shuram excursion, if recording a large perturbation in the carbon cycle, provides an excellent window into the feedback between carbon, oxygen and nitrogen cycles in deep time. However, the role of the nitrogen cycle in the Shuram excursion has not been systematically investigated. Kikumoto et al. (2014) reported nitrogen isotope data from the Ediacaran to early Cambrian in a drill core in the Yangtze Gorges area, South China, and found a coherent decrease in  $\delta^{15}\text{N}$  along with the Shuram excursion in the upper Doushantuo Formation (Locally named as N3, EN3 or DOUNCE, Jiang et al., 2007; Zhou and Xiao, 2007; Zhu et al., 2013). This negative  $\delta^{15}\text{N}$  excursion was interpreted as evidence for an increased nitrate pool which may have resulted in the partial assimilation of  $\text{NO}_3^-$  (Kikumoto et al., 2014; Nishizawa et al., 2019). Nitrogen isotope data have also been reported from the other Ediacaran sections in South China and other continents (e.g., Ader et al., 2014; Spangenberg et al., 2014; Wang et al., 2017; Chen et al., 2019; Lan et al., 2019; Nishizawa et al., 2019), but the Shuram excursion is poorly developed or missing in these sections. In this contribution, we report high resolution  $\delta^{15}\text{N}$  and  $\delta^{13}\text{C}_{\text{org}}$  data from the upper Doushantuo Formation in two sections (Jiulongwan and Xiangerwan) in the Yangtze Gorges area, South China, where the Shuram-EN3 excursion is well recorded (Jiang et al., 2007; An et al., 2015; Zhou et al., 2017). The new data presented here, along with previous ones, will shed new light on the origin of the Shuram excursion and the coevolution of carbon and nitrogen cycles during this critical interval.



## GEOLOGICAL SETTING AND STUDY SECTIONS

The Ediacaran Doushantuo Formation was deposited in an inferred passive continental margin setting along the southeast part of the South China Block, following the termination of the Marinoan glaciation (Wang and Li, 2003; Jiang et al., 2011). In the Yangtze Gorges area, western Hubei Province, the Doushantuo Formation in the stratotype (Jiulongwan) section can be divided into four lithological members: Member I is a 3–5 m thick cap carbonate, Member II is characterized by interlayered black shale and muddy limestone with abundant centimeter-scaled chert nodules, Member III is dominated by carbonate deposits, and Member IV consists mainly of black shales with meter-scale carbonate concretions (e.g., Jiang et al., 2011). Abundant microfossils and macrofossils have been reported from the Doushantuo Formation, providing a unique window into eukaryotic evolution leading up to the Cambrian Explosion, as well as a valuable tool for biostratigraphic subdivision (Liu et al., 2014; Xiao et al., 2016; Zhou et al., 2019 and references therein).

Geochronologically, the depositional age of the Doushantuo Formation has previously been constrained to ca. 635–551 Ma based on U-Pb zircon dating (Condon et al., 2005; Zhang et al., 2005). Regional stratigraphic correlation suggest that the ca. 551 Ma tuffaceous layer within the Miaohe Member, which was traditionally correlated with Member IV, is likely located in the overlying Dengying Formation (An et al., 2015), implying that the upper boundary of the Doushantuo Formation is older than 551 Ma. However, a more detailed investigation of  $\delta^{13}C_{carb}$  of multiple sections around the Huangling Anticline (Zhou et al., 2017) and the  $\delta^{13}C_{org}$  study from the Miaohe member (Xiao et al., 2017) argue against the correlation scheme proposed by An et al. (2015).

Our samples were collected from the upper part of the Doushantuo Formation in the Jiulongwan and Xiangerwan sections in the Yangtze Gorges area (Figure 1). These two sections were chosen for nitrogen isotope analyses due to the excellent preservation of the Shuram-EN3 carbon isotope excursion (Jiang et al., 2007; An et al., 2015; Zhou et al., 2017). Paleogeographically, the two sections were both

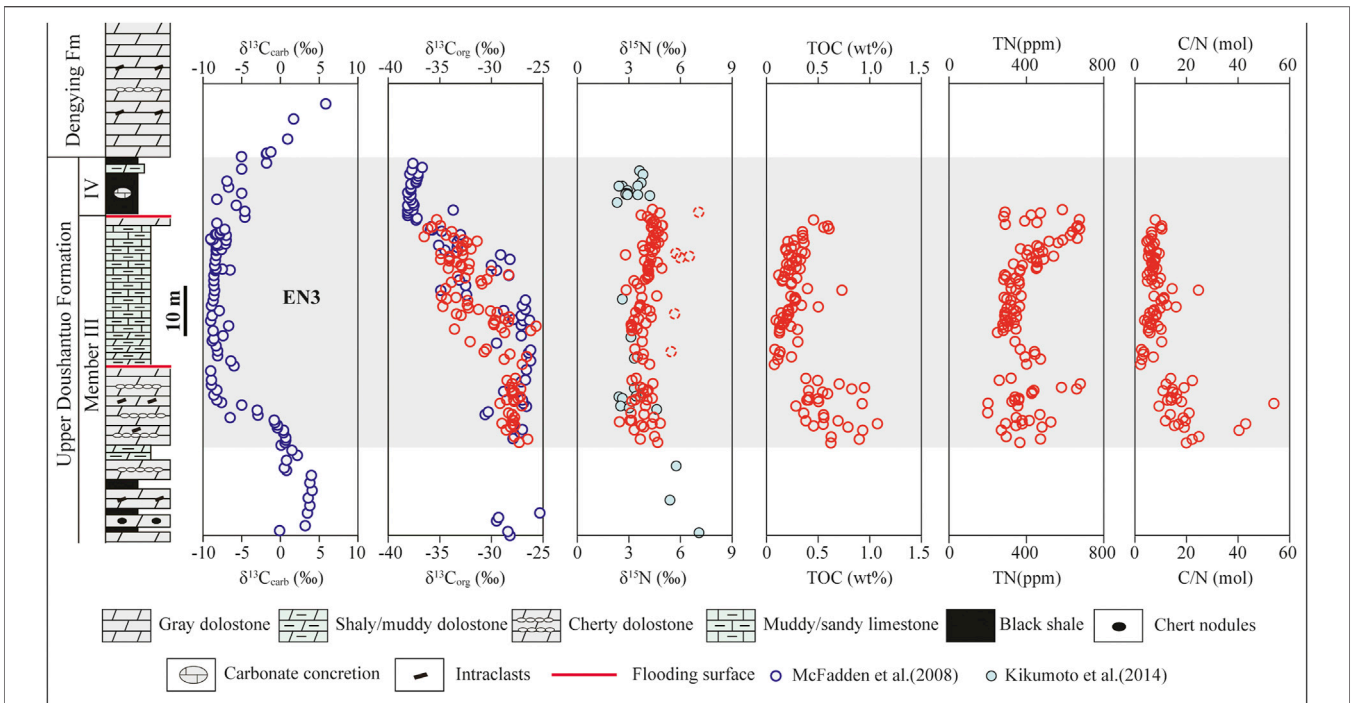


**FIGURE 2 |** The geochemical profiles of  $\delta^{13}C_{carb}$ ,  $\delta^{13}C_{org}$ ,  $\delta^{15}N$ , TOC, TN and MC/N spanning the Shuram-EN3 excursion in the Jiulongwan section. The data points with dashed outline fall away from the general trend.

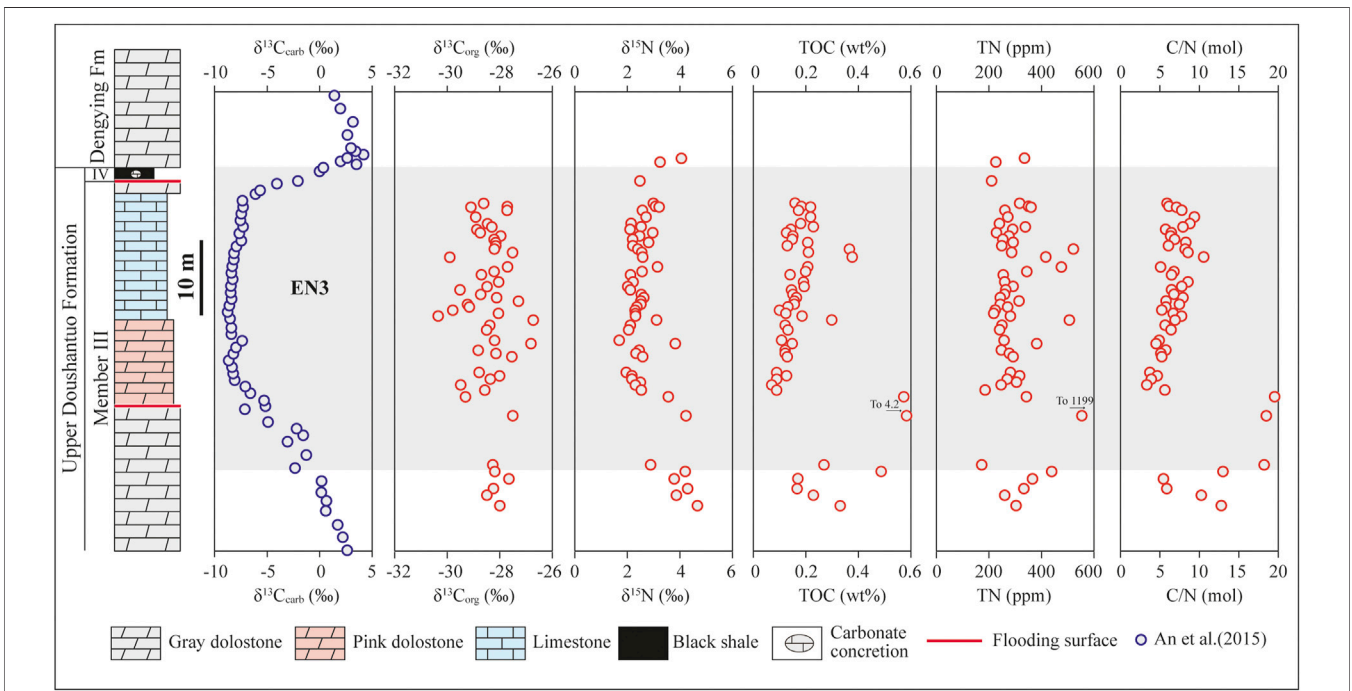


**FIGURE 3 |** The geochemical profiles of  $\delta^{13}C_{carb}$ ,  $\delta^{13}C_{org}$ ,  $\delta^{15}N$ , TOC, TN and MC/N spanning the Shuram-EN3 excursion in the Xiangerwan section.

deposited in proximal settings of an intrashelf basin (Jiang et al., 2011; An et al., 2015). The Jiulongwan section, located in the southern part of the Huangling Anticline (Figure 1), has been extensively studied to characterize the ocean redox structure (e.g., Jiang et al., 2007; McFadden et al., 2008; Li et al., 2010; Zhou et al., 2012; Ling et al., 2013; Wei et al., 2018; Fan et al., 2020, 2021). The upper Doushantuo Formation in the Jiulongwan section is dominated by cherty dolostone, muddy limestone/dolostone and black shales (Figure 2). The Shuram-EN3 excursion begins in the middle part of Member III, continued upwards through the rest of the Doushantuo Formation until return to positive  $\delta^{13}\text{C}_{\text{carb}}$  values at the Doushantuo/Dengying boundary (Figure 2). The Xiangerwan section is located in the northwestern part of the Huangling Anticline (Figure 1), about 60 km away from the Jiulongwan section. The upper Doushantuo Formation in this section is mainly composed of medium-thick bedded dolostone, pink dolostone and thinly bedded limestone with subordinate black shales (Figure 3). The pink dolostone was interpreted as the precipitate of a primary marine red bed enabled by ocean oxygenation (Song et al., 2017). The pattern of the Shuram-EN3 excursion in the Xiangerwan section is similar to that of the Jiulongwan section (Figure 3).

## ANALYTICAL METHOD

We performed measurements of  $\delta^{15}\text{N}$  and  $\delta^{13}\text{C}_{\text{org}}$ , total nitrogen (TN) contents, and total organic carbon (TOC) contents for 162 samples. Fresh sample chips without any weathering surfaces or visible veins were ground into powders below 200 mesh in an agate mortar. About 10 g of powders from each sample were treated with 2 M excess HCl to ensure the complete removal of carbonate. The carbonate-free samples were then rinsed with deionized water multiple times until a near-neutral pH value was reached. After centrifuging, the decarbonated sample residue was dried at 70°C in an oven before analysis. The isotopic and elemental compositions were measured in the Oxy-Anion Stable Isotope Consortium (OASIC) at Louisiana State University (LSU), using a Vario Microcube Elemental Analyzer (EA) connected to an Isoprime 100 isotope ratio mass spectrometer (IRMS). Because most of our samples are TOC-lean carbonate rocks, approximately 50–100 mg sample powders (based on TOC estimation) were wrapped in tin capsules and combusted in the EA to enhance the N signal. The organic carbon isotope compositions are reported as  $\delta$  values with reference to the Vienna Pee Dee Belemnite standard (VPDB). The nitrogen isotope compositions are reported in standard  $\delta$  notation in per mil (‰) deviations from atmospheric  $\text{N}_2$  (0‰, Air). Reference standard acetanilide-OASIC ( $\delta^{13}\text{C} = -27.62\text{‰}$ ,  $\delta^{15}\text{N} = +1.61\text{‰}$ ) was used to calibrate the analytical results. Measurements of C and N concentrations of blanks were below detection limits, suggesting that contamination from capsules did not contribute much to our results. A few samples ( $n = 10$ ) with N peaks much lower than that of the reference standard were excluded from the dataset and from the discussion. The reproducibility monitored by the reference material was better than 0.1‰ for  $\delta^{13}\text{C}_{\text{org}}$  and 0.3‰ for  $\delta^{15}\text{N}$ .

## RESULTS

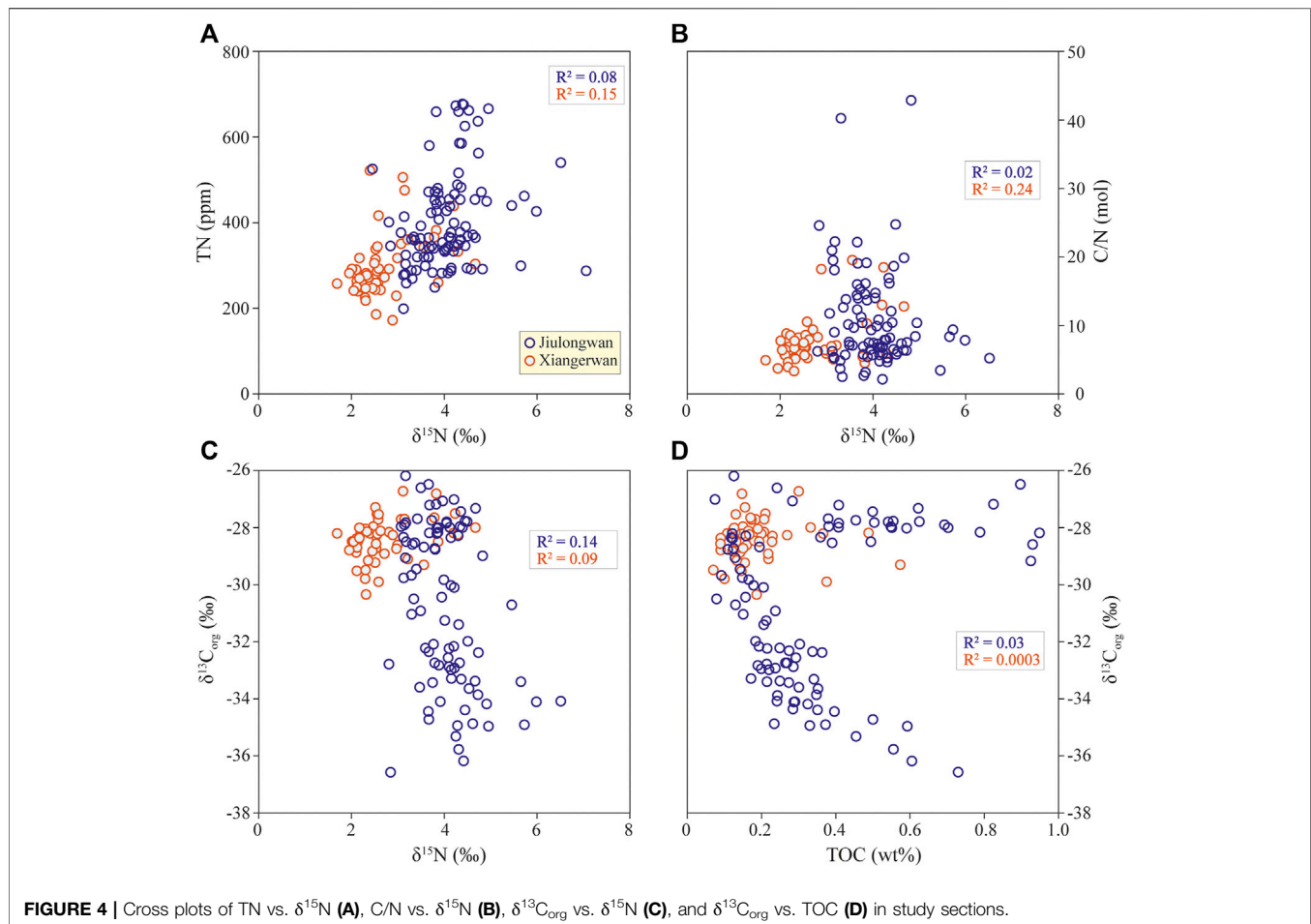
The analytical results of  $\delta^{15}\text{N}$ ,  $\delta^{13}\text{C}_{\text{org}}$ , TN, TOC and C/N are shown in Figures 2, 3 and Supplementary Tables S1, S2. The  $\delta^{13}\text{C}_{\text{org}}$  variations in the Jiulongwan section are well matched with previously published data by McFadden et al. (2008) (Figure 2). In the prelude and lower part of the Shuram-EN3 excursion,  $\delta^{13}\text{C}_{\text{org}}$  is relatively high and centers around  $-28\text{‰}$ . It becomes more variable but shows an overall decreasing trend in the rest of Member III. Low and stable  $\delta^{13}\text{C}_{\text{org}}$  values cluster around  $-38\text{‰}$  in the Member IV black shale. The  $\delta^{15}\text{N}$  data of our samples in the Jiulongwan section largely overlap with those reported from the equivalent interval in the nearby (within 3 km) Wuhe drillcore (Figure 2; Kikumoto et al., 2014). Before the Shuram-EN3 excursion, a few data points show relatively high  $\delta^{15}\text{N}$  values from  $+5.4\text{‰}$  to  $+6.7\text{‰}$ . During the main phase of the Shuram-EN3 excursion, most of  $\delta^{15}\text{N}$  values fall in the range of  $+3\text{‰}$  to  $+5.5\text{‰}$ , except for a few outliers, with an average of  $+3.8 \pm 0.8\text{‰}$  ( $n = 123$ ) (Figure 2; this study; Kikumoto et al., 2014). The variability in  $\delta^{15}\text{N}$  is independent of lithological changes.

In the Xiangerwan section,  $\delta^{13}\text{C}_{\text{org}}$  does not show any clear stratigraphic trend across the Shuram-EN3 excursion. It varies between  $-30.3\text{‰}$  and  $-26.7\text{‰}$ , with an average of  $-28.4 \pm 0.7\text{‰}$  ( $n = 49$ ) (Figure 3). Variations in  $\delta^{15}\text{N}$  from this section generally mirror the trend of  $\delta^{13}\text{C}_{\text{carb}}$  reported by An et al. (2015), although the magnitude of change is small (Figure 3). Prior to the Shuram-EN3 excursion,  $\delta^{15}\text{N}$  varies from  $+3.0\text{‰}$  to  $+4.7\text{‰}$  and the mean value is  $+4.0 \pm 0.6\text{‰}$  ( $n = 6$ ). During the main stage of excursion, most samples have  $\delta^{15}\text{N}$  values between  $+2.0\text{‰}$  and  $+3.8\text{‰}$ . The average value ( $+2.5 \pm 0.4\text{‰}$ ,  $n = 43$ ) is about 1.5‰ lower than that of the pre-excursion interval. An increase of  $\delta^{15}\text{N}$  relative to pre-excursion values is observed in the upper Doushantuo Formation, coincident with the rising branch of the Shuram-EN3 excursion. Overall, the  $\delta^{15}\text{N}$  values from the Xiangerwan section are 1–2‰ lower than those from the Jiulongwan section.

## DISCUSSION

### Evaluation of the Preservation of Primary Isotopic Signals

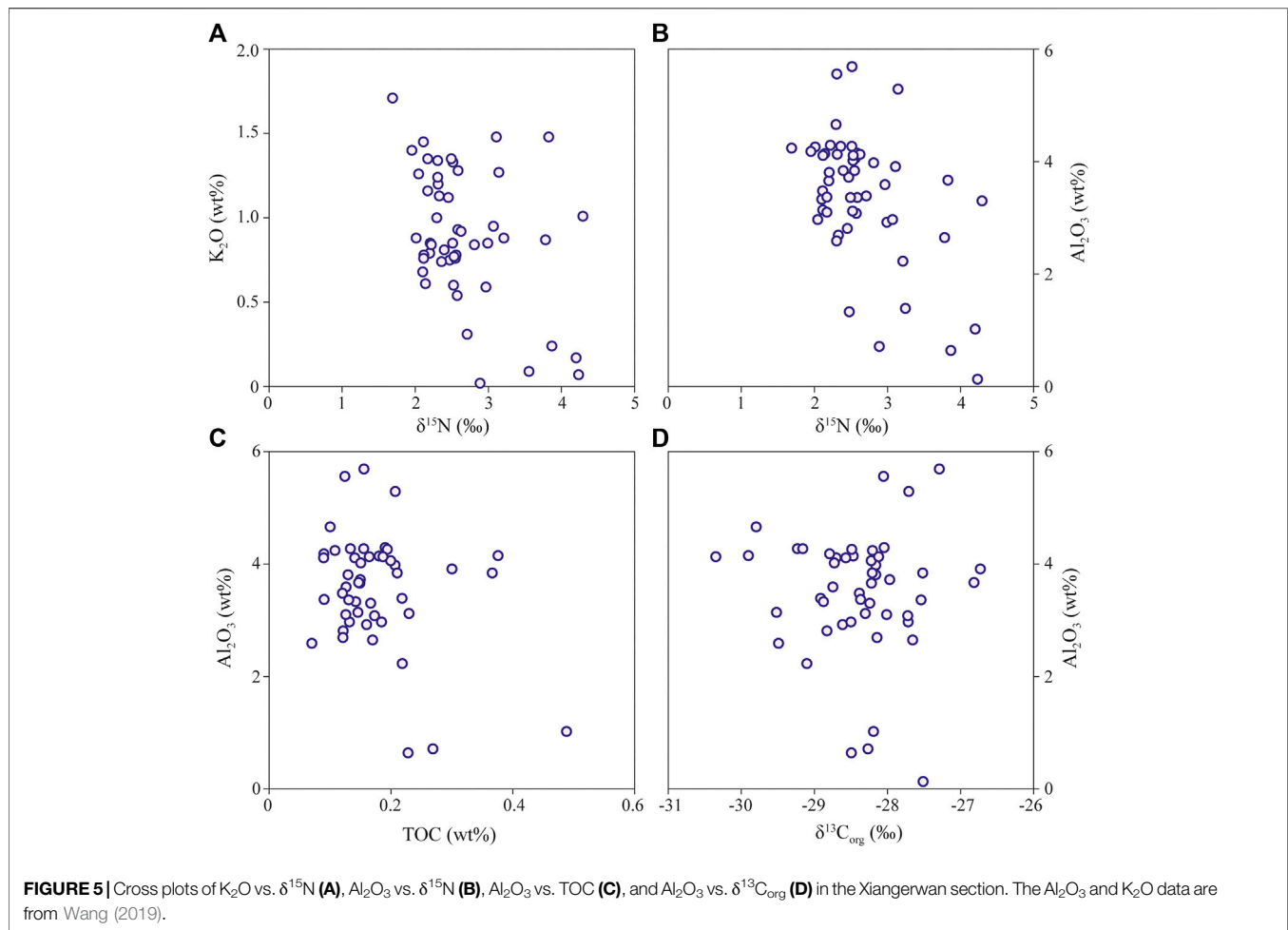
Whether  $\delta^{15}\text{N}$  and  $\delta^{13}\text{C}_{\text{org}}$  in sedimentary rocks record primary autochthonous signatures is dependent on several factors, including paleogeographic setting, diagenesis, metamorphism, and potential contributions of allochthonous materials (Ader et al., 2009; Ader et al., 2016; Robinson et al., 2012; Stüeken et al., 2016). In modern oceans, sedimentary  $\delta^{15}\text{N}$  of organic matter may show large offsets compared to sinking organic particles at sites located off continental margins due to extended remineralization of organic matter in the water column and upper sediment. In contrast, on continental shelves with high sediment accumulation rates and/or organic matter content, sedimentary organic matter generally displays  $\delta^{15}\text{N}$  values similar to that of sinking particles (Robinson et al., 2012). The two study sections were deposited in shallow shelf environments (Jiang et al., 2011; An et al., 2015), minimizing this



effect on sedimentary  $\delta^{15}\text{N}$  as well as  $\delta^{13}\text{C}_{\text{org}}$ . However subsequent biological decomposition and thermal maturation of sedimentary organic matter during early and burial diagenesis can still perturb the original  $\delta^{15}\text{N}$  and  $\delta^{13}\text{C}_{\text{org}}$  values (Ader et al., 2009; Ader et al., 2016; Stüeken et al., 2016). Several lines of evidence, however, argue against these processes as major controls on our data. First, the isotopic alteration by biological decomposition during early diagenesis is generally small for  $\delta^{13}\text{C}_{\text{org}}$  (Ader et al., 2009 and references therein). Although this effect could be large for  $\delta^{15}\text{N}$  (up to 4‰) when bottom water was oxic (Altabet et al., 1999; Freudenthal et al., 2001; Lehmann et al., 2002; Prokopenko et al., 2006), Fe speciation data,  $I/(\text{Ca} + \text{Mg})$  ratios and Ce anomalies ( $\text{Ce}/\text{Ce}^*$ ) from the Jiulongwan and Xiangerwan sections indicate oxygen-depleted bottom water conditions (Li et al., 2010; Zhou et al., 2012; Ling et al., 2013; Wei et al., 2019). Second, Raman spectra and equivalent vitrinite reflectance data suggested that the peak heating temperature of the Doushantuo Formation was  $<300^\circ\text{C}$  (Chang et al., 2020), and at such low metamorphic grade thermal alterations of isotopic composition would be limited for both  $\delta^{15}\text{N}$  and  $\delta^{13}\text{C}_{\text{org}}$  (Ader et al., 2009; Ader et al., 2016; Stüeken et al., 2016; Stüeken et al., 2017). Lastly, if the original  $\delta^{13}\text{C}_{\text{org}}$  and  $\delta^{15}\text{N}$  were largely modified by the preferential loss of light  $^{12}\text{C}$  and/or  $^{14}\text{N}$  during early and burial diagenesis, one would expect

correlation between  $\delta^{15}\text{N}$ , TN, C/N, and  $\delta^{13}\text{C}_{\text{org}}$  as well as  $\delta^{13}\text{C}_{\text{org}}$  and TOC. No significant correlations, however, are observed between these parameters (Figure 4). A subset of samples show a negative correlation between  $\delta^{13}\text{C}_{\text{org}}$  and TOC commonly seen in Precambrian rocks, but the reason of this is unknown based on current research and warrants further investigation.

The addition of material from allochthonous sources is another factor that can affect sedimentary  $\delta^{13}\text{C}_{\text{org}}$  and  $\delta^{15}\text{N}$ . These allochthonous sources include hydrothermal fluids and detrital input. Hydrothermal fluids are unlikely to increase the organic carbon to sedimentary rocks, but they could contain some inorganic N that can be trapped by sedimentary clay when moving along the fractures, thereby affecting the bulk  $\delta^{15}\text{N}$  (e.g., Zerkle et al., 2017; Luo et al., 2018). However, no clear correlation is observed between potassium abundance (Wang, 2019) and  $\delta^{15}\text{N}$  and in the Xiangerwan section (Figure 5A), suggesting that exchange with hydrothermal fluids was limited and did not severely bias our  $\delta^{15}\text{N}$  values. For sedimentary rocks with low authigenic TOC contents, detrital organic matter could be a major component and overprint the primary  $\delta^{13}\text{C}_{\text{org}}$  (Jiang et al., 2010). It is difficult to quantify the contribution of detrital organic matter and detrital clay-bound N to our samples; however,  $\delta^{15}\text{N}$ ,  $\delta^{13}\text{C}_{\text{org}}$  and TOC do not show



correlations with Al content in the Xiangerwan section (Wang, 2019)—an indicator of detrital input (**Figures 5B–D–D**). Therefore, we suggest that detrital input did not significantly affect our data. Nevertheless, this question can be further clarified in a future dedicated study.

### Variations of $\delta^{15}N$ - $\delta^{13}C_{carb}$ Pattern in the Upper Doushantuo Formation

The upper Doushantuo Formation in South China is characterized by a prominent negative  $\delta^{13}C_{carb}$  excursion (N3, EN3 or DOUNCE) that is widely accepted to be equivalent to the Shuram excursion (Jiang et al., 2007; Zhou and Xiao, 2007; Zhu et al., 2007; Zhu et al., 2013; McFadden et al., 2008; Wang et al., 2012; Lu et al., 2013; An et al., 2015; Wang et al., 2016; Li et al., 2017; Zhou et al., 2017; Wei et al., 2019). Although the Shuram-EN3 excursion has a wide paleogeographic distribution from the inner shelf to upper slope setting, it shows large spatial variations in its pattern, magnitude and stratigraphic coverage (Wang et al., 2016; Zhou et al., 2017). In some sections, this excursion is completely absent (Zhou et al., 2017). The discrepancy of the Shuram-EN3 excursion between different sections has been attributed to facies change, stratigraphic truncation, the

diachronous nature of the Doushantuo/Dengying boundary and/or diagenetic overprinting of primary isotope signatures (Cui et al., 2015; Wang et al., 2016; Zhou et al., 2017).

$\delta^{15}N$  data for the Ediacaran Doushantuo Formation were first reported from the Wuhe drillcore in Yangtze Gorges area by Kikumoto et al. (2014). They found a synchronous decrease in  $\delta^{15}N$  from ca. +6‰ to ca. +3.2‰ along with the Shuram-EN3 excursion (**Figure 6B**; Kikumoto et al., 2014). Our new  $\delta^{15}N$  data from the upper Doushantuo Formation in the Jiulongwan section, which is <3 km away from the Wuhe drillcore, are well consistent with the trend reported by Kikumoto et al. (2014) when excluding a few outliers (**Figure 6B**). In the inner shelf Xiangerwan section about 60 km north of the Jiulongwan section, the Shuram-EN3 excursion is well developed and shows striking similarity with that in the Jiulongwan section (**Figure 6A**; An et al., 2015). The  $\delta^{15}N$  data also mirror the trend observed in the Wuhe drillcore, although the absolute values are overall 1–2‰ lower than those of the Wuhe drillcore both before and during the Shuram-EN3 excursion. The  $\delta^{15}N$ - $\delta^{13}C_{carb}$  pattern from the upper Doushantuo Formation in the outer shelf Wangjiapeng drillcore section shows some differences compared to the Wuhe (Jiulongwan) and Xiangerwan sections (**Figure 6C**; Lan et al., 2019). The Shuram-EN3 excursion in this

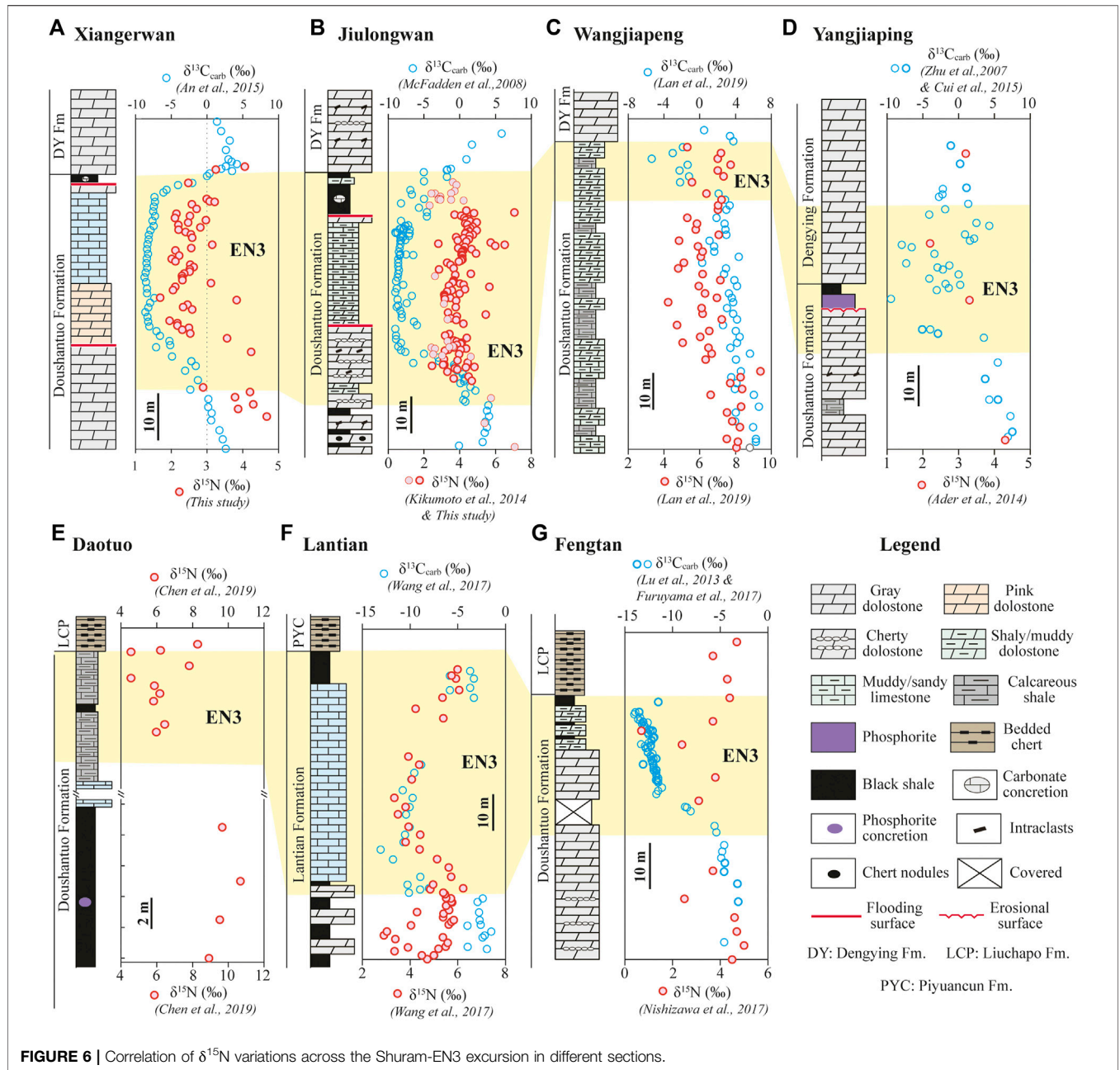


**FIGURE 6 |** Correlation of  $\delta^{15}\text{N}$  variations across the Shuram-EN3 excursion in different sections.

section is marked by a sharp decrease of  $\delta^{13}\text{C}_{\text{carb}}$  to a minimum value of  $-5.4\text{‰}$ , followed by a quick return to positive values, while the associated  $\delta^{15}\text{N}$  in this interval shows an opposite (increasing) trend. It should be noted that  $\delta^{15}\text{N}$  in the Wangjiapeng section shows a small negative excursion in the ‘uppermost’ Doushantuo Formation, clearly postdating the Shuram-EN3 excursion (Lan et al., 2019). Whether this negative  $\delta^{15}\text{N}$  excursion can be correlated with that in the Wuhe and Xiangerwan sections is questionable and requires further investigation.

In the Yangjiaping section on the shelf margin, Ediacaran  $\delta^{13}\text{C}_{\text{carb}}$  data were reported by several research groups (Zhu et al., 2007; Ader et al., 2009; Kunimitsu et al., 2011; Cui et al., 2015).

Here the Shuram-EN3 excursion spans the upper Doushantuo Formation and the lower part of the overlying Dengying Formation, but the data show large sample-to-sample variations (Wang et al., 2016). A few  $\delta^{15}\text{N}$  data points from this interval show a decreasing trend from  $\sim +4.3\text{‰}$  to  $\sim +3.0\text{‰}$  (Figure 6D; Ader et al., 2014). More data are needed to confirm this variation. Chen et al. (2019) reported  $\delta^{15}\text{N}$  data from the Doushantuo Formation in an upper slope drill core section (zk 2012) in the Daotuo area, northeastern Guizhou Province. A conspicuous decline in  $\delta^{15}\text{N}$  was observed in the upper Doushantuo Formation (Figure 6E; Chen et al., 2019). Although no  $\delta^{13}\text{C}_{\text{carb}}$  data were reported in zk 2012, the  $\delta^{13}\text{C}_{\text{carb}}$  profile from an adjacent drill core verifies the

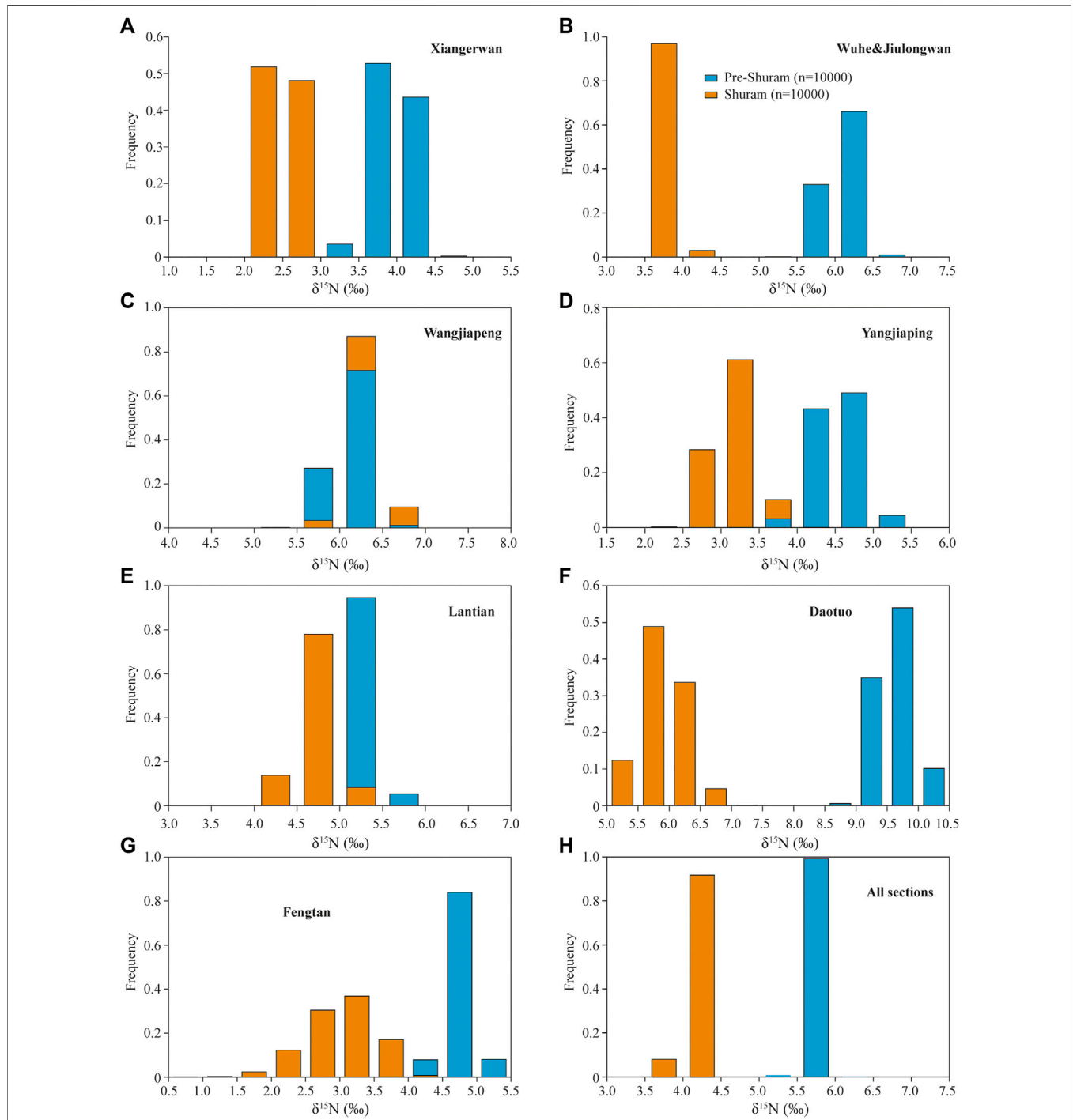


**FIGURE 7 |** Bootstrap distribution of  $\delta^{15}\text{N}$  before and during the Shuram-EN3 excursion in the Xiangerean section (A), Jiulongwan section (B), Wangjiapeng drill core (C), Yangjiaping section (D), Lantian drill core (E), Daotuo drill core (F), Fengtan section (G), and all sections (H).

presence of the Shuram-EN3 excursion in the upper Doushantuo Formation (Wei et al., 2019). Coupled  $\delta^{15}\text{N}$ - $\delta^{13}\text{C}_{\text{carb}}$  data have also been reported from the Lantian Formation in southern Anhui, which is equivalent to the Doushantuo Formation (Wang et al., 2017). The  $\delta^{13}\text{C}_{\text{carb}}$  from this unit is dominated by negative values and show a negative excursion in the upper

Lantian Formation that is considered to be correlative to the Shuram excursion. However, the  $\delta^{15}\text{N}$  data from this interval do not show a clear stratigraphic trend (Figure 6F; Wang et al., 2017). In the basinal Fengtan section, the Shuram-EN3 excursion is documented in the upper Doushantuo Formation (Figure 6G; Lu et al., 2013; Furuyama et al., 2017). In the same interval, the

$\delta^{15}\text{N}$  also show a clear decreasing trend from  $\sim +4.5\text{‰}$  to nadir  $+0.7\text{‰}$  (Figure 6G; Nishizawa et al., 2019). Recently, a  $\delta^{15}\text{N}$  study was performed for the Doushantuo Formation in the proximal E-Shan section (Peng et al., 2020). However, this section is not included in our correlation (Figure 6) because the Doushantuo Formation is dominated by siliciclastic rocks and do not contain the Shuram excursion.

To better characterize the overall  $\delta^{15}\text{N}$  trend during this critical time interval, we simulate the  $\delta^{15}\text{N}$  variations before and during the Shuram excursion for each section using a bootstrap resampling method. Out of seven sections, six sections are characterized by a bimodal  $\delta^{15}\text{N}$  distribution (Figure 7). Notably, although the  $\delta^{15}\text{N}$  data from the Lantian section do not show a clear stratigraphic trend (Wang et al., 2017), the model result indicates that  $\delta^{15}\text{N}$  during the Shuram excursion are statistically  $0.6\text{‰}$  lower than prior to the excursion (Figure 7E). In the Wangjiapeng section, the mean  $\delta^{15}\text{N}$  distributions obtained from bootstrap resampling largely overlap for pre- and syn-excursion strata (Figure 7C). This is likely due to a prominent negative  $\delta^{15}\text{N}$  excursion in the lower part of the Doushantuo Formation (Lan et al., 2019). The bimodal  $\delta^{15}\text{N}$  distribution becomes even more evident when the bootstrap method is applied to all data from the seven sections (Figure 7H), providing evidence for a synchronous decrease of  $\delta^{15}\text{N}$  associated with the Shuram excursion. This covariation pattern could be attributed to a feedback between nitrogen and carbon cycles that will be discussed in the following section.

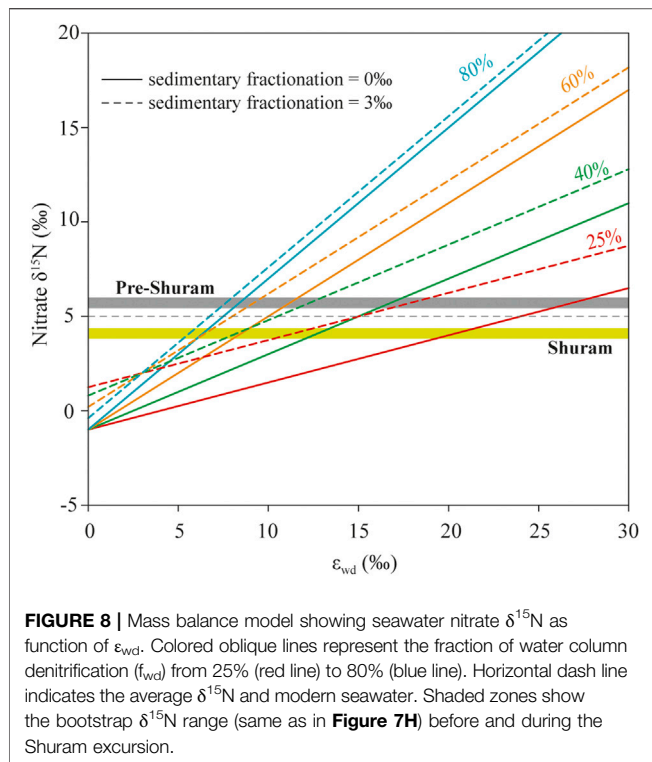
## Feedback Between Nitrogen and Carbon Cycles

Modeled results indicate that  $\delta^{15}\text{N}$  data from the Ediacaran Doushantuo Formation show contrasting distributions before and during the Shuram excursion (Figure 7). High  $\delta^{15}\text{N}$  values from the lower-middle Doushantuo Formation prior to the Shuram excursion have been attributed to incomplete denitrification that preferentially removed light  $^{14}\text{N}$  from the ocean (Kikumoto et al., 2014; Ader et al., 2014; Wang et al., 2017, 2018; Chen et al., 2019; Lan et al., 2019; Xu et al., 2020). The decrease of  $\delta^{15}\text{N}$  associated with the Shuram excursion was previously interpreted as partial assimilation of  $\text{NO}_3^-$  from an expanding nitrate pool in response to a rise of oxygen levels in the ocean-atmosphere system, implying that dissolved P rather than N was the limiting nutrient during the excursion interval (Kikumoto et al., 2014; Nishizawa et al., 2019). We challenge this explanation for the following reasons. First, if the decrease in  $\delta^{15}\text{N}$  was caused by partial assimilation of  $\text{NO}_3^-$ , the  $^{15}\text{N}$ -enriched residual  $\text{NO}_3^-$  would be quantitatively utilized in other parts of the basin. One should expect a positive  $\delta^{15}\text{N}$  excursion in the upper Doushantuo Formation in some sections, which, however, has not been observed in sections studied to date (Figure 7); Second, the upper Doushantuo Formation contains abundant phosphatized fossils and phosphorite deposits (Xiao et al., 1998; Xiao et al., 2014; Liu et al., 2014; She et al., 2014; Yin et al., 2015; Zhang Y. et al., 2019), possibly indicating high dissolved P level in coeval seawater (e.g., Laakso et al., 2020). Thus, it is unlikely that P was severely limited during the Shuram excursion.

Alternatively, the isotopic shift could have been caused by a shift in the location of denitrification changes in the relative proportions of water column denitrification vs. sedimentary denitrification can affect the seawater  $\delta^{15}\text{N}$  and accordingly sedimentary  $\delta^{15}\text{N}$  (Sigman et al., 2009; Algeo et al., 2014; Stüeken et al., 2016). In the modern oceans, water column denitrification accounts for 25–32% of total denitrification and is generally accompanied by large isotope fractionation ( $\epsilon \approx \delta^{15}\text{N}_{\text{reactant}} - \delta^{15}\text{N}_{\text{product}}$ ). The remaining 68–75% of denitrification occurs within sedimentary porewaters with small or negligible isotope fractionation. The balance between these two processes and  $\text{N}_2$  fixation determines the isotope composition of modern seawater (average ca.  $+5\text{‰}$ ) (Sigman et al., 2009; Algeo et al., 2014; Stüeken et al., 2016). Assuming a steady isotope scenario, a high fraction of water column denitrification would thus increase the  $\delta^{15}\text{N}$  of seawater nitrate, and vice versa (Sigman et al., 2009; Algeo et al., 2014; Stüeken et al., 2016). Hence, the decrease of  $\delta^{15}\text{N}$  coupled with the Shuram excursion on the Yangtze Platform could have resulted from the decrease of the fraction of water column denitrification. This requires a more widely oxygenated ocean than today, i.e. a complete absence of oxygen minimum zones, which is not supported by any current geochemical and geological evidence. However, the nitrogen isotope mass balance can potentially also be affected by sea level. Algeo et al. (2014) compiled  $\delta^{15}\text{N}$  data from the Cryogenian to present and found a long-term decrease in  $\delta^{15}\text{N}$  from the Cryogenian to the Cambrian, which they attributed to a first-order climate-driven sea level change. According to this model, high eustatic sea level could have resulted in relatively low  $\delta^{15}\text{N}$  if the dominant locus of denitrification shifted to sediments (Algeo et al., 2014). However, this model is difficult to reconcile with the relatively stable positive  $\delta^{15}\text{N}$  values from ca. 750 Ma to 570 Ma, spanning from the Tonian through the Cryogenian to the middle Ediacaran (Ader et al., 2014). Particularly, after the deglaciation of the Marinoan Snowball Earth, which represented a global sea level rise,  $\delta^{15}\text{N}$  remains high for at least 60 Myr or even longer until the onset of the Shuram excursion (Xiang et al., 2018; Chen et al., 2019; Xu et al., 2020). Further, from the Ediacaran to early Cambrian the ocean was characterized by predominately anoxic environments with multiple short-term oxygenation events (Sahoo et al., 2016; Li et al., 2018). Under such conditions, the fraction of water column denitrification should always have been much higher than it is in more oxygenated oceans like today, even during intervals of high eustatic sea level. Therefore, changes in proportion of water column denitrification alone cannot readily explain the decrease in  $\delta^{15}\text{N}$  during the Shuram excursion.

Variation in the isotope fractionation associated with water column denitrification is another factor that can modulate seawater  $\delta^{15}\text{N}$ . According to the mass balance model for the nitrogen cycle (Sigman et al., 2009; Algeo et al., 2014; Stüeken et al., 2016), the seawater nitrate  $\delta^{15}\text{N}$  is determined by the isotopic balance between input and output processes, which can be described in the following formulation:

$$\delta^{15}\text{N}_{\text{atmosphere}} - \epsilon_{\text{fix}} = \delta^{15}\text{N}_{\text{nitrate}} - \epsilon_{\text{den}} \quad (1)$$



where  $\epsilon_{fix}$  refers to isotopic fractionation of  $\text{N}_2$  fixation, and  $\epsilon_{den}$  represents net isotope fractionation of total denitrification which can be expressed as:

$$\epsilon_{den} = f_{wd} \cdot \epsilon_{wd} + (1 - f_{wd}) \cdot \epsilon_{sd} \quad (2)$$

where the subscripts *wd* and *sd* refer to water column denitrification and sedimentary denitrification, respectively, and  $f_{wd}$  represents the fraction of water column denitrification. In modern oceans, the  $\epsilon_{wd}$  can vary from 0‰ for quantitative denitrification to 30‰ (Sigman et al., 2009 and references therein). To model seawater nitrate  $\delta^{15}\text{N}$  as a function of  $\epsilon_{wd}$ , we set  $\epsilon_{fix}$  to be +1‰ and  $\epsilon_{sd}$  to be 0‰ (Sigman et al., 2009 and references therein). If the fraction of water column denitrification was 25% during the Ediacaran as generally suggested for today (Sigman et al., 2009), the mean  $\delta^{15}\text{N}$  of pre-Shuram samples corresponds to  $\epsilon_{wd}$  of 26–28%, and the decrease of  $\delta^{15}\text{N}$  during the Shuram excursion would require a decrease of  $\epsilon_{wd}$  to 19–21% (**Figure 8**). The  $\epsilon_{wd}$  could have been smaller if  $f_{wd}$  increased (**Figure 8**). For example,  $\epsilon_{wd}$  for the mean  $\delta^{15}\text{N}$  of the Shuram interval would be 12–13‰, if  $f_{wd}$  increased to 40%, and it would decrease to ca. 6‰ when increasing  $f_{wd}$  to 80%. A high fraction of  $f_{wd}$  was possible for the Ediacaran when anoxic marine environments were more extensive than today. Modifying  $\epsilon_{sd}$  to 3‰ as observed in some modern sediment (Kessler et al., 2014) would require a lower  $\epsilon_{wd}$  to produce the same  $\delta^{15}\text{N}$ . This difference would be large when  $f_{wd}$  was low but small as  $f_{wd}$  increased (**Figure 8**).

As discussed above, the decrease of  $\delta^{15}\text{N}$  associated with the Shuram excursion can be well explained by the decrease of  $\epsilon_{wd}$ . We argue that this change may have been caused by a feedback between the nitrogen and carbon cycles at that time. Enhanced

continental weathering before the Shuram excursion, as evidenced by the increase of  $^{87}\text{Sr}/^{86}\text{Sr}$  (Sawaki et al., 2010; Wang et al., 2014; Cui et al., 2015; Xiao et al., 2016; Lan et al., 2019), would have delivered substantial amounts of nutrients to the ocean, promoting primary productivity (Williams et al., 2019). High primary productivity would have resulted in an expansion of anoxic bottom waters on productive continental shelves. These anoxic waters would have been capped by oxic surface waters, leading to extensive aerobic respiration or organic matter along the redox interface. An ensuing consequence of this combined effect would have been the significant consumption of nitrate through enhanced denitrification. Stoichiometric relationships indicate that remineralization of 1 mol of organic carbon through denitrification would consume 85 mol or even more nitrate (Altabet, 2006). The shrinkage of the nitrate pool may have reduced  $\epsilon_{wd}$  due to reservoir effects, as has been documented from modern microbial cultures, where  $\epsilon_{wd}$  decreased when nitrate levels dropped to a few  $\mu\text{M}$  (compared to  $\sim 30 \mu\text{M}$  in the modern open ocean) (Kritee et al., 2012). Additionally, the decrease of nitrate levels would inevitably shift the nitrogen cycle towards  $\text{N}_2$  fixation and ammonium assimilation, which may also partially contribute to the lower  $\delta^{15}\text{N}$  during the Shuram excursion, as evidenced by a near zero value observed in the Fengtan section (Nishizawa et al., 2019). In the long time scale, an increase in organic burial in the context of high primary productivity would have led to rising  $\text{O}_2$  levels (e.g., Alcott et al., 2019). This inference is consistent with the increase of  $\text{I}/(\text{Ca} + \text{Mg})$  ratios (Hardisty et al., 2017; Wei et al., 2019), a large positive  $\delta^{238}\text{U}$  excursion (Zhang F. et al., 2019; Cao et al., 2020), and a negative excursion of thallium isotope composition ( $\epsilon^{205}\text{Tl}$ ) (Fan et al., 2020) during the Shuram interval. The rise of oxygen would have resulted in partial oxidation of dissolved organic carbon stored in the anoxic deep ocean (Rothman et al., 2003) or of other forms of reduced carbon (e.g., Bjerrum and Canfield, 2011), lowering the  $\delta^{13}\text{C}$  of inorganic carbon in seawater, as documented in the Shuram excursion. Further, the recycled N and P from the oxidation of organic matter could have been upwelled to the photic zone, providing new nutrient input for organisms and further stimulating primary productivity. Although we cannot completely rule out the possibility of diagenetic overprint over the Shuram signal in individual cases, the coupled variations of  $\delta^{13}\text{C}_{carb}$  and  $\delta^{15}\text{N}$  in multiple sections across the Yangtze Platform suggest that they may partially record changes in primary seawater signals in response to the complex feedback between carbon and nitrogen cyclings during this critical period.

## CONCLUSION

High resolution  $\delta^{15}\text{N}$  and  $\delta^{13}\text{C}_{org}$  data are reported from the upper part of the Ediacaran Doushantuo Formation in two well-preserved sections in the Yangtze Gorges area, South China. These data, coupled with previously published  $\delta^{13}\text{C}_{carb}$  in the same sections, are used to elucidate the inherent relationship between carbon and nitrogen cycling during the Shuram-EN3 excursion—the deepest negative  $\delta^{13}\text{C}_{carb}$  excursion in Earth history. The  $\delta^{15}\text{N}$  data in the studied sections show concurrent variations with  $\delta^{13}\text{C}_{carb}$ , although the magnitude of change is much smaller. Bootstrapping simulations

further demonstrate a clear decrease of  $\delta^{15}\text{N}$  associated with the Shuram-EN3 excursion. We argue that the decrease in  $\delta^{15}\text{N}$  during the Shuram-EN3 excursion can be reasonably explained by the reduction of isotopic fractionation associated with water column denitrification rather than the partial assimilation of nitrate. The parallel changes in  $\delta^{13}\text{C}_{\text{carb}}$  and  $\delta^{15}\text{N}$  may have resulted from feedbacks between carbon and nitrogen cycles.

## DATA AVAILABILITY STATEMENT

The original contributions presented in the study are included in the article/**Supplementary Material**, further inquiries can be directed to the corresponding author.

## AUTHOR CONTRIBUTIONS

XW and XS designed research. DX and XW collected samples. DX, XW, and YP performed lab analyses. XW, DX, XS, YP, and ES wrote the paper.

## REFERENCES

- Ader, M., Macouin, M., Trindade, R. I. F., Hadrien, M.-H., Yang, Z., Sun, Z., et al. (2009). A Multilayered Water Column in the Ediacaran Yangtze Platform? Insights from Carbonate and Organic Matter Paired  $\delta^{13}\text{C}$ . *Earth Planet. Sci. Lett.* 288, 213–227. doi:10.1016/j.epsl.2009.09.024
- Ader, M., Sansjofre, P., Halverson, G. P., Busigny, V., Trindade, R. I. F., Kunzmann, M., et al. (2014). Ocean Redox Structure across the Late Neoproterozoic Oxygenation Event: A Nitrogen Isotope Perspective. *Earth Planet. Sci. Lett.* 396, 1–13. doi:10.1016/j.epsl.2014.03.042
- Ader, M., Thomazo, C., Sansjofre, P., Busigny, V., Papineau, D., Laffont, R., et al. (2016). Interpretation of the Nitrogen Isotopic Composition of Precambrian Sedimentary Rocks: Assumptions and Perspectives. *Chem. Geol.* 429, 93–110. doi:10.1016/j.chemgeo.2016.02.010
- Alcott, L. J., Mills, B. J. W., and Poulton, S. W. (2019). Stepwise Earth Oxygenation Is an Inherent Property of Global Biogeochemical Cycling. *Science* 366, 1333–1337. doi:10.1126/science.aax6459
- Algeo, T. J., Meyers, P. A., Robinson, R. S., Rowe, H., and Jiang, G. Q. (2014). Icehouse-greenhouse Variations in marine Denitrification. *Biogeosciences* 11, 1273–1295. doi:10.5194/bg-11-1273-2014
- Altabet, M. A. (2006). "Isotopic Tracers of the Marine Nitrogen Cycle: Present and Past," in *Marine Organic Matter: Biomarkers, Isotopes and DNA. The Handbook of Environmental Chemistry, Vol 2N*. Editor J.K. Volkman (Berlin, Heidelberg: Springer), 251–293. doi:10.1007/698\_2\_008
- Altabet, M. A., Pilskaln, C., Thunell, R., Pride, C., Sigman, D., Chavez, F., et al. (1999). The Nitrogen Isotope Biogeochemistry of Sinking Particles from the Margin of the Eastern North Pacific. *Deep Sea Res. Oceanographic Res. Pap.* 46, 655–679. doi:10.1016/S0967-0637(98)00084-3
- An, Z., Jiang, G., Tong, J., Tian, L., Ye, Q., Song, H., et al. (2015). Stratigraphic Position of the Ediacaran Miaohu Biota and its Constrains on the Age of the Upper Doushantuo  $\delta^{13}\text{C}$  Anomaly in the Yangtze Gorges Area, South China. *Precambrian Res.* 271, 243–253. doi:10.1016/j.precamres.2015.10.007
- Bjerrum, C. J., and Canfield, D. E. (2011). Towards a Quantitative Understanding of the Late Neoproterozoic Carbon Cycle. *Proc. Natl. Acad. Sci.* 108, 5542–5547. doi:10.1073/pnas.1101755108
- Bowring, S. A., Grotzinger, J. P., Condon, D. J., Ramezani, J., Newall, M. J., and Allen, P. A. (2007). Geochronologic Constraints on the Chronostratigraphic Framework of the Neoproterozoic Huqf Supergroup, Sultanate of Oman. *Am. J. Sci.* 307, 1097–1145. doi:10.2475/10.2007.01

## FUNDING

This research is supported by the National Natural Science Foundation of China (41872032, 41830215, 41930320) and the Chinese '111' project (B20011).

## ACKNOWLEDGMENTS

Haoming Wei and Lijing Wang participated part of field trip and sample collection. We are indebted to Hao Yan for the kind help with the carbon and nitrogen isotope analyses. Thanks are given to two reviewers for valuable comments that improve the quality of this paper.

## SUPPLEMENTARY MATERIAL

The Supplementary Material for this article can be found online at: <https://www.frontiersin.org/articles/10.3389/feart.2021.678149/full#supplementary-material>

- Bristow, T. F., and Kennedy, M. J. (2008). Carbon Isotope Excursions and the Oxidant Budget of the Ediacaran Atmosphere and Ocean. *Geol* 36, 863–866. doi:10.1130/g24968a.1
- Burns, S. J., and Matter, A. (1993). Carbon Isotopic Record of the Latest Proterozoic from Oman. *Eclogae Geologicae Helv.* 86, 595–607.
- Canfield, D. E., Knoll, A. H., Poulton, S. W., Narbonne, G. M., and Dunning, G. R. (2020). Carbon Isotopes in Clastic Rocks and the Neoproterozoic Carbon Cycle. *Am. J. Sci.* 320, 97–124. doi:10.2475/02.2020.01
- Cao, M., Daines, S. J., Lenton, T. M., Cui, H., Algeo, T. J., Dahl, T. W., et al. (2020). Comparison of Ediacaran platform and slope  $\delta^{238}\text{U}$  records in South China: Implications for global-ocean oxygenation and the origin of the Shuram Excursion. *Geochimica et Cosmochimica Acta* 287, 111–124. doi:10.1016/j.gca.2020.04.035
- Chang, B., Li, C., Liu, D., Foster, I., Tripati, A., Lloyd, M. K., et al. (2020). Massive Formation of Early Diagenetic Dolomite in the Ediacaran Ocean: Constraints on the "Dolomite Problem". *Proc. Natl. Acad. Sci. USA* 117, 14005–14014. doi:10.1073/pnas.1916673117
- Chen, Y., Diamond, C. W., Stüeken, E. E., Cai, C., Gill, B. C., Zhang, F., et al. (2019). Coupled Evolution of Nitrogen Cycling and Redoxcline Dynamics on the Yangtze Block across the Ediacaran-Cambrian Transition. *Geochimica et Cosmochimica Acta* 257, 243–265. doi:10.1016/j.gca.2019.05.017
- Condon, D., Zhu, M. Y., Bowring, S., Wang, W., Yang, A. H., and Jin, Y. G. (2005). U-pb Ages from the Neoproterozoic Doushantuo Formation, China. *Science* 308, 95–98. doi:10.1126/science.1107765
- Cui, H., Kaufman, A. J., Xiao, S., Zhou, C., and Liu, X.-M. (2017). Was the Ediacaran Shuram Excursion a Globally Synchronized Early Diagenetic Event? Insights from Methane-Derived Authigenic Carbonates in the Uppermost Doushantuo Formation, South China. *Chem. Geol.* 450, 59–80. doi:10.1016/j.chemgeo.2016.12.010
- Cui, H., Kaufman, A. J., Xiao, S., Zhu, M., Zhou, C., and Liu, X.-M. (2015). Redox Architecture of an Ediacaran Ocean Margin: Integrated Chemostratigraphic ( $\delta^{13}\text{C}$ - $\Delta^{34}\text{S}$ - $^{87}\text{Sr}/^{86}\text{Sr}$ - $^{86}\text{Sr}/\text{Ce}$ - $^{87}\text{Sr}/\text{Ce}$ ) Correlation of the Doushantuo Formation, South China. *Chem. Geol.* 405, 48–62. doi:10.1016/j.chemgeo.2015.04.009
- Derry, L. A. (2010). A Burial Diagenesis Origin for the Ediacaran Shuram-Wonoka Carbon Isotope Anomaly. *Earth Planet. Sci. Lett.* 294, 152–162. doi:10.1016/j.epsl.2010.03.022
- Devol, A. H. (2015). Denitrification, Anammox, and  $\text{N}_2$  Production in Marine Sediments. *Annu. Rev. Mar. Sci.* 7, 403–423. doi:10.1146/annurev-marine-010213-135040
- Falkowski, P. G. (1997). Evolution of the Nitrogen Cycle and its Influence on the Biological Sequestration of  $\text{CO}_2$  in the Ocean. *Nature* 387, 272–275. doi:10.1038/387272a0

- Fan, H., Fu, X., Ward, J. F., Yin, R., Wen, H., and Feng, X. (2021). Mercury Isotopes Track the Cause of Carbon Perturbations in the Ediacaran Ocean. *Geol.* 49, 248–252. doi:10.1130/g48266.1
- Fan, H., Nielsen, S. G., Owens, J. D., Auro, M., Shu, Y., Hardisty, D. S., et al. (2020). Constraining Oceanic Oxygenation during the Shuram Excursion in South China Using Thallium Isotopes. *Geobiol.* 18, 348–365. doi:10.1111/gbi.12379
- Fennel, K., Follows, M., and Falkowski, P. G. (2005). The Co-evolution of the Nitrogen, Carbon and Oxygen Cycles in the Proterozoic Ocean. *Am. J. Sci.* 305, 526–545. doi:10.2475/ajs.305.6-8.526
- Fike, D. A., Grotzinger, J. P., Pratt, L. M., and Summons, R. E. (2006). Oxidation of the Ediacaran Ocean. *Nature* 444, 744–747. doi:10.1038/nature05345
- Freudenthal, T., Wagner, T., Wenzhöfer, F., Zabel, M., and Wefer, G. (2001). Early Diagenesis of Organic Matter from Sediments of the Eastern Subtropical Atlantic: Evidence from Stable Nitrogen and Carbon Isotopes. *Geochimica et Cosmochimica Acta* 65, 1795–1808. doi:10.1016/S0016-7037(01)00554-3
- Furuyama, S., Kano, A., Kunimitsu, Y., Ishikawa, T., Wang, W., and Liu, X. (2017). Chemostratigraphy of the Ediacaran Basinal Setting on the Yangtze Platform, South China: Oceanographic and Diagenetic Aspects of the Carbon Isotopic Depth Gradient. *Isl. Arc* 26, e12196. doi:10.1111/iar.12196
- Gong, Z., and Li, M. (2020). Astrochronology of the Ediacaran Shuram Carbon Isotope Excursion, Oman. *Earth Planet. Sci. Lett.* 547, 116462. doi:10.1016/j.epsl.2020.116462
- Grotzinger, J. P., Fike, D. A., and Fischer, W. W. (2011). Enigmatic Origin of the Largest-Known Carbon Isotope Excursion in Earth's History. *Nat. Geosci.* 4, 285–292. doi:10.1038/ngeo1138
- Halverson, G. P., Wade, B. P., Hurtgen, M. T., and Barovich, K. M. (2010). Neoproterozoic Chemostratigraphy. *Precambrian Res.* 182, 337–350. doi:10.1016/j.precamres.2010.04.007
- Hardisty, D. S., Lu, Z., Bekker, A., Diamond, C. W., Gill, B. C., Jiang, G., et al. (2017). Perspectives on Proterozoic Surface Ocean Redox from Iodine Contents in Ancient and Recent Carbonate. *Earth Planet. Sci. Lett.* 463, 159–170. doi:10.1016/j.epsl.2017.01.032
- Higgins, M. B., Robinson, R. S., Husson, J. M., Carter, S. J., and Pearson, A. (2012). Dominant Eukaryotic export Production during Ocean Anoxic Events Reflects the Importance of Recycled NH<sub>4</sub><sup>+</sup>. *Proc. Natl. Acad. Sci.* 109, 2269–2274. doi:10.1073/pnas.1104313109
- Husson, J. M., Linzmeier, B. J., Kitajima, K., Ishida, A., Maloof, A. C., Schoene, B., et al. (2020). Large Isotopic Variability at the Micron-Scale in 'Shuram' Excursion Carbonates from South Australia. *Earth Planet. Sci. Lett.* 538, 116211. doi:10.1016/j.epsl.2020.116211
- Husson, J. M., Maloof, A. C., Schoene, B., Chen, C. Y., and Higgins, J. A. (2015). Stratigraphic Expression of Earth's Deepest  $\delta^{13}\text{C}$  Excursion in the Wonoka Formation of South Australia. *Am. J. Sci.* 315, 1–45. doi:10.2475/01.2015.01
- Jiang, G., Kaufman, A. J., Christie-Blick, N., Zhang, S., and Wu, H. (2007). Carbon Isotope Variability across the Ediacaran Yangtze Platform in South China: Implications for a Large Surface-To-Deep Ocean  $\delta^{13}\text{C}$  Gradient. *Earth Planet. Sci. Lett.* 261, 303–320. doi:10.1016/j.epsl.2007.07.009
- Jiang, G., Shi, X., Zhang, S., Wang, Y., and Xiao, S. (2011). Stratigraphy and Paleogeography of the Ediacaran Doushantuo Formation (Ca. 635–551Ma) in South China. *Gondwana Res.* 19, 831–849. doi:10.1016/j.gr.2011.01.006
- Jiang, G., Wang, X., Shi, X., Zhang, S., Xiao, S., and Dong, J. (2010). Organic Carbon Isotope Constraints on the Dissolved Organic Carbon (DOC) Reservoir at the Cryogenian-Ediacaran Transition. *Earth Planet. Sci. Lett.* 299, 159–168. doi:10.1016/j.epsl.2010.08.031
- Jiang, L., Planavsky, N., Zhao, M., Liu, W., and Wang, X. (2019). Authigenic Origin for a Massive Negative Carbon Isotope Excursion. *Geol.* 47, 115–118. doi:10.1130/g45709.1
- Kaufman, A. J., Corsetti, F. A., and Varni, M. A. (2007). The Effect of Rising Atmospheric Oxygen on Carbon and Sulfur Isotope Anomalies in the Neoproterozoic Johnnie Formation, Death Valley, USA. *Chem. Geol.* 237, 47–63. doi:10.1016/j.chemgeo.2006.06.023
- Kessler, A. J., Bristow, L. A., Cardenas, M. B., Glud, R. N., Thamdrup, B., and Cook, P. L. M. (2014). The Isotope Effect of Denitrification in Permeable Sediments. *Geochimica et Cosmochimica Acta* 133, 156–167. doi:10.1016/j.gca.2014.02.029
- Kikumoto, R., Tahata, M., Nishizawa, M., Sawaki, Y., Maruyama, S., Shu, D., et al. (2014). Nitrogen Isotope Chemostratigraphy of the Ediacaran and Early Cambrian Platform Sequence at Three Gorges, South China. *Gondwana Res.* 25, 1057–1069. doi:10.1016/j.gr.2013.06.002
- Knauth, L. P., and Kennedy, M. J. (2009). The Late Precambrian Greening of the Earth. *Nature* 460, 728–732. doi:10.1038/nature08213
- Kritee, K., Sigman, D. M., Granger, J., Ward, B. B., Jayakumar, A., and Deutsch, C. (2012). Reduced Isotope Fractionation by Denitrification under Conditions Relevant to the Ocean. *Geochimica et Cosmochimica Acta* 92, 243–259. doi:10.1016/j.gca.2012.05.020
- Kump, L. R., and Arthur, M. A. (1999). Interpreting Carbon-Isotope Excursions: Carbonates and Organic Matter. *Chem. Geol.* 161, 181–198. doi:10.1016/S0009-2541(99)00086-8
- Kump, L. R., Junium, C., Arthur, M. A., Brasier, A., Fallick, A., Melezhik, V., et al. (2011). Isotopic Evidence for Massive Oxidation of Organic Matter Following the Great Oxidation Event. *Science* 334, 1694–1696. doi:10.1126/science.1213999
- Kunimitsu, Y., Setsuda, Y., Furuyama, S., Wang, W., Kano, A., et al. (2011). Ediacaran chemostratigraphy and paleoceanography at a shallow marine setting in northwestern Hunan Province, South China. *Precambrian Res.* 191, 194–208. doi:10.1016/j.precamres.2011.09.006
- Laakso, T. A., Sperling, E. A., Johnston, D. T., and Knoll, A. H. (2020). Ediacaran Reorganization of the marine Phosphorus Cycle. *Proc. Natl. Acad. Sci. USA* 117, 11961–11967. doi:10.1073/pnas.1916738117
- Lam, P., and Kuypers, M. M. M. (2011). Microbial Nitrogen Cycling Processes in Oxygen Minimum Zones. *Annu. Rev. Mar. Sci.* 3, 317–345. doi:10.1146/annurev-marine-120709-142814
- Lan, Z., Sano, Y., Yahagi, T., Tanaka, K., Shirai, K., Papineau, D., et al. (2019). An Integrated Chemostratigraphic ( $\delta^{13}\text{C}$ - $\Delta^{18}\text{O}$ - $87\text{Sr}/86\text{Sr}$ - $\Delta^{15}\text{N}$ ) Study of the Doushantuo Formation in Western Hubei Province, South China. *Precambrian Res.* 320, 232–252. doi:10.1016/j.precamres.2018.10.018
- Le Guerroué, E., Allen, P. A., and Cozzi, A. (2006a). Chemostratigraphic and Sedimentological Framework of the Largest Negative Carbon Isotopic Excursion in Earth History: The Neoproterozoic Shuram Formation (Nafun Group, Oman). *Precambrian Res.* 146, 68–92. doi:10.1016/j.precamres.2006.01.007
- Le Guerroué, E., Allen, P. A., Cozzi, A., Etienne, J. L., and Fanning, M. (2006b). 50 Myr Recovery from the Largest negative  $\delta^{13}\text{C}$  Excursion in the Ediacaran Ocean. *Terra Nova* 18, 147–153. doi:10.1111/j.1365-3121.2006.00674.x
- Lee, C., Love, G. D., Fischer, W. W., Grotzinger, J. P., and Halverson, G. P. (2015). Marine Organic Matter Cycling during the Ediacaran Shuram Excursion. *Geol.* 43, 1106. doi:10.1130/g37236.1
- Lehmann, M. F., Bernasconi, S. M., Barbieri, A., and McKenzie, J. A. (2002). Preservation of Organic Matter and Alteration of its Carbon and Nitrogen Isotope Composition during Simulated and *In Situ* Early Sedimentary Diagenesis. *Geochimica et Cosmochimica Acta* 66, 3573–3584. doi:10.1016/S0016-7037(02)00968-7
- Li, C., Cheng, M., Zhu, M., and Lyons, T. W. (2018). Heterogeneous and Dynamic marine Shelf Oxygenation and Coupled Early Animal Evolution. *Emerging Top. Life Sci.* 2, 279–288. doi:10.1042/ets20170157
- Li, C., Hardisty, D. S., Luo, G., Huang, J., Algeo, T. J., Cheng, M., et al. (2017). Uncovering the Spatial Heterogeneity of Ediacaran Carbon Cycling. *Geobiol.* 15, 211–224. doi:10.1111/gbi.12222
- Li, C., Love, G. D., Lyons, T. W., Fike, D. A., Sessions, A. L., and Chu, X. (2010). A Stratified Redox Model for the Ediacaran Ocean. *Science* 328, 80–83. doi:10.1126/science.1182369
- Ling, H.-F., Chen, X., Li, D., Wang, D., Shields-Zhou, G. A., and Zhu, M. (2013). Cerium Anomaly Variations in Ediacaran-Earliest Cambrian Carbonates from the Yangtze Gorges Area, South China: Implications for Oxygenation of Coeval Shallow Seawater. *Precambrian Res.* 225, 110–127. doi:10.1016/j.precamres.2011.10.011
- Liu, P., Xiao, S., Yin, C., Chen, S., Zhou, C., and Li, M. (2014). Ediacaran Acanthomorphic Acritarchs and Other Microfossils from Chert Nodules of the Upper Doushantuo Formation in the Yangtze Gorges Area, South China. *J. Paleontol.* 88, 1–139. doi:10.1666/13-009
- Lu, M., Zhu, M., Zhang, J., Shields-Zhou, G., Li, G., Zhao, F., et al. (2013). The DOUNCE Event at the Top of the Ediacaran Doushantuo Formation, South China: Broad Stratigraphic Occurrence and Non-diagenetic Origin. *Precambrian Res.* 225, 86–109. doi:10.1016/j.precamres.2011.10.018
- Luo, G., Junium, C. K., Izon, G., Ono, S., Beukes, N. J., Algeo, T. J., et al. (2018). Nitrogen Fixation Sustained Productivity in the Wake of the Palaeoproterozoic Great Oxidation Event. *Nat. Commun.* 9, 978. doi:10.1038/s41467-018-03361-2
- Lyons, T. W., Reinhard, C. T., and Planavsky, N. J. (2014). The Rise of Oxygen in Earth's Early Ocean and Atmosphere. *Nature* 506, 307–315. doi:10.1038/nature13068

- McFadden, K. A., Huang, J., Chu, X., Jiang, G., Kaufman, A. J., Zhou, C., et al. (2008). Pulsed Oxidation and Biological Evolution in the Ediacaran Doushantuo Formation. *Proc. Natl. Acad. Sci.* 105, 3197–3202. doi:10.1073/pnas.0708336105
- Melezhik, V., Fallick, A., Pokrovsky, B. G., and Pokrovsky, B. (2005). Enigmatic Nature of Thick Sedimentary Carbonates Depleted in C beyond the Canonical Mantle Value: The Challenges to Our Understanding of the Terrestrial Carbon Cycle. *Precambrian Res.* 137, 131–165. doi:10.1016/j.precamres.2005.03.010
- Michiels, C. C., Darchambeau, F., Roland, F. A. E., Morana, C., Llíros, M., García-Armisen, T., et al. (2017). Iron-dependent Nitrogen Cycling in a Ferruginous lake and the Nutrient Status of Proterozoic Oceans. *Nat. Geosci.* 10, 217–221. doi:10.1038/ngeo2886
- Nishizawa, M., Tsuchiya, Y., Du, W., Sawaki, Y., Matsui, Y., Wang, Y., et al. (2019). Shift in Limiting Nutrients in the Late Ediacaran-Early Cambrian marine Systems of South China. *Palaeogeogr. Palaeoclimatol. Palaeoecol.* 530, 281–299. doi:10.1016/j.palaeo.2019.05.036
- Paulsen, T., Deering, C., Sliwinski, J., Bachmann, O., and Guillong, M. (2017). Evidence for a Spike in Mantle Carbon Outgassing during the Ediacaran Period. *Nat. Geosci.* 10, 930–934. doi:10.1038/s41561-017-0011-6
- Peng, Y., Dong, L., Ma, H., Wang, R., Lang, X., Peng, Y., et al. (2020). Surface Ocean Nitrate-Limitation in the Aftermath of Marinoan Snowball Earth: Evidence from the Ediacaran Doushantuo Formation in the Western Margin of the Yangtze Block, South China. *Precambrian Res.* 347, 105846. doi:10.1016/j.precamres.2020.105846
- Prokopenko, M., Hammond, D., Berelson, W., Bernhard, J., Stott, L., and Douglas, R. (2006). Nitrogen Cycling in the Sediments of Santa Barbara basin and Eastern Subtropical North Pacific: Nitrogen Isotopes, Diagenesis and Possible Chemosymbiosis between Two Lithotrophs (Thioploca and Anammox)-"riding on a Glider". *Earth Planet. Sci. Lett.* 242, 186–204. doi:10.1016/j.epsl.2005.11.044
- Quan, T. M., Wright, J. D., and Falkowski, P. G. (2013). Co-variation of Nitrogen Isotopes and Redox States through Glacial-Interglacial Cycles in the Black Sea. *Geochimica Et Cosmochimica Acta* 112, 305–320. doi:10.1016/j.gca.2013.02.029
- Robinson, R. S., Kienast, M., Luiza Albuquerque, A., Altabet, M., Contreras, S., De Pol Holz, R., et al. (2012). A Review of Nitrogen Isotopic Alteration in marine Sediments. *Paleoceanography* 27, PA4203. doi:10.1029/2012pa002321
- Rooney, A. D., Cantine, M. D., Bergmann, K. D., Gómez-Pérez, I., Al Baloushi, B., Boag, T. H., et al. (2020). Calibrating the Coevolution of Ediacaran Life and Environment. *Proc. Natl. Acad. Sci. USA* 117, 16824–16830. doi:10.1073/pnas.2002918117
- Rothman, D. H., Hayes, J. M., and Summons, R. E. (2003). Dynamics of the Neoproterozoic Carbon Cycle. *Pnas* 100, 8124–8129. doi:10.1073/pnas.0832439100
- Sahoo, S. K., Planavsky, N. J., Jiang, G., Kendall, B., Owens, J. D., Wang, X., et al. (2016). Oceanic Oxygenation Events in the Anoxic Ediacaran Ocean. *Geobiol.* 14, 457–468. doi:10.1111/gbi.12182
- Sawaki, Y., Ohno, T., Tahata, M., Komiya, T., Hirata, T., Maruyama, S., et al. (2010). The Ediacaran Radiogenic Sr Isotope Excursion in the Doushantuo Formation in the Three Gorges Area, South China. *Precambrian Res.* 176, 46–64. doi:10.1016/j.precamres.2009.10.006
- Schrag, D. P., Higgins, J. A., Macdonald, F. A., and Johnston, D. T. (2013). Authigenic Carbonate and the History of the Global Carbon Cycle. *Science* 339, 540–543. doi:10.1126/science.1229578
- She, Z.-B., Strother, P., and Papineau, D. (2014). Terminal Proterozoic Cyanobacterial Blooms and Phosphogenesis Documented by the Doushantuo Granular Phosphorites II: Microbial Diversity and C Isotopes. *Precambrian Res.* 251, 62–79. doi:10.1016/j.precamres.2014.06.004
- Shi, W., Li, C., Luo, G., Huang, J., Algeo, T. J., Jin, C., et al. (2018). Sulfur Isotope Evidence for Transient marine-shelf Oxidation during the Ediacaran Shuram Excursion. *Geol.* 46, 267–270. doi:10.1130/G39663.1
- Shields, G. A., Mills, B. J. W., Zhu, M., Raub, T. D., Daines, S. J., and Lenton, T. M. (2019). Unique Neoproterozoic Carbon Isotope Excursions Sustained by Coupled Evaporite Dissolution and Pyrite Burial. *Nat. Geosci.* 12, 823–827. doi:10.1038/s41561-019-0434-3
- Sigman, D. M., Casciotti, K. L., and Casciotti, K. L. (2001). "Nitrogen Isotopes in the Ocean," in *Encyclopedia of Ocean Science* (Amsterdam: Elsevier), 1884–1894. doi:10.1006/rwos.2001.0172
- Song, H., Jiang, G., Poulton, S. W., Wignall, P. B., Tong, J., Song, H., et al. (2017). The Onset of Widespread marine Red Beds and the Evolution of Ferruginous Oceans. *Nat. Commun.* 8, 399. doi:10.1038/s41467-017-00502-x
- Spangenberg, J. E., Bagnoud-Velásquez, M., Boggiani, P. C., and Gaucher, C. (2014). Redox Variations and Bioproductivity in the Ediacaran: Evidence from Inorganic and Organic Geochemistry of the Corumbá Group, Brazil. *Gondwana Res.* 26, 1186–1207. doi:10.1016/j.gr.2013.08.014
- Stüeken, E. E., Kipp, M. A., Koehler, M. C., and Buick, R. (2016). The Evolution of Earth's Biogeochemical Nitrogen Cycle. *Earth-Science Rev.* 160, 220–239. doi:10.1016/j.earscirev.2016.07.007
- Stüeken, E. E., Zaloumis, J., Meixnerová, J., and Buick, R. (2017). Differential Metamorphic Effects on Nitrogen Isotopes in Kerogen Extracts and Bulk Rocks. *Geochimica et Cosmochimica Acta* 217, 80–94. doi:10.1016/j.gca.2017.08.019
- Sui, Y., Huang, C., Zhang, R., Wang, Z., and Ogg, J. (2019). Astronomical Time Scale for the Middle-Upper Doushantuo Formation of Ediacaran in South China: Implications for the Duration of the Shuram/Wonoka Negative  $\delta^{13}\text{C}$  Excursion. *Palaeogeogr. Palaeoclimatol. Palaeoecol.* 532, 109273. doi:10.1016/j.palaeo.2019.109273
- Swart, P. K., and Kennedy, M. J. (2012). Does the Global Stratigraphic Reproducibility of  $\delta^{13}\text{C}$  in Neoproterozoic Carbonates Require a marine Origin? A Pliocene-Pleistocene Comparison. *Geol.* 40, 87–90. doi:10.1130/g32538.1
- Tyrrell, T. (1999). The Relative Influences of Nitrogen and Phosphorus on Oceanic Primary Production. *Nature* 400, 525–531. doi:10.1038/22941
- Wang, J., and Li, Z.-X. (2003). History of Neoproterozoic Rift Basins in South China: Implications for Rodinia Break-Up. *Precambrian Res.* 122, 141–158. doi:10.1016/S0301-9268(02)00209-7
- Wang, L. (2019). *Variations of Trace Elements in the Upper Part of the Ediacaran Doushantuo Formation and Environmental Implication*. Beijing: China University of Geosciences. Master Thesis (in Chinese with English abstract). doi:10.1130/abs/2019am-336558
- Wang, W., Guan, C., Zhou, C., Peng, Y., Pratt, L. M., Chen, X., et al. (2017). Integrated Carbon, Sulfur, and Nitrogen Isotope Chemostratigraphy of the Ediacaran Lantian Formation in South China: Spatial Gradient, Ocean Redox Oscillation, and Fossil Distribution. *Geobiol.* 15, 552–571. doi:10.1111/gbi.12226
- Wang, W., Zhou, C., Guan, C., Yuan, X., Chen, Z., and Wan, B. (2014). An Integrated Carbon, Oxygen, and Strontium Isotopic Studies of the Lantian Formation in South China with Implications for the Shuram Anomaly. *Chem. Geol.* 373, 10–26. doi:10.1016/j.chemgeo.2014.02.023
- Wang, W., Zhou, C., Yuan, X., Chen, Z., and Xiao, S. (2012). A Pronounced Negative  $\delta^{13}\text{C}$  Excursion in an Ediacaran Succession of Western Yangtze Platform: A Possible Equivalent to the Shuram Event and its Implication for Chemostratigraphic Correlation in South China. *Gondwana Res.* 22, 1091–1101. doi:10.1016/j.gr.2012.02.017
- Wang, X., Jiang, G., Shi, X., Peng, Y., and Morales, D. C. (2018). Nitrogen Isotope Constraints on the Early Ediacaran Ocean Redox Structure. *Geochimica et Cosmochimica Acta* 240, 220–235. doi:10.1016/j.gca.2018.08.034
- Wang, X., Jiang, G., Shi, X., and Xiao, S. (2016). Paired Carbonate and Organic Carbon Isotope Variations of the Ediacaran Doushantuo Formation from an Upper Slope Section at Siduping, South China. *Precambrian Res.* 273, 53–66. doi:10.1016/j.precamres.2015.12.010
- Wei, H., Wang, X., Shi, X., Jiang, G., Tang, D., Wang, L., et al. (2019). Iodine Content of the Carbonates from the Doushantuo Formation and Shallow Ocean Redox Change on the Ediacaran Yangtze Platform, South China. *Precambrian Res.* 322, 160–169. doi:10.1016/j.precamres.2019.01.007
- Wei, W., Frei, R., Gilleaudeau, G. J., Li, D., Wei, G.-Y., Chen, X., et al. (2018). Oxygenation Variations in the Atmosphere and Shallow Seawaters of the Yangtze Platform during the Ediacaran Period: Clues from Cr-Isotope and Ce-Anomaly in Carbonates. *Precambrian Res.* 313, 78–90. doi:10.1016/j.precamres.2018.05.009
- Williams, J. J., Mills, B. J. W., and Lenton, T. M. (2019). A Tectonically Driven Ediacaran Oxygenation Event. *Nat. Commun.* 10, 2690. doi:10.1038/s41467-019-10286-x
- Xiang, L., Schoepfer, S. D., Zhang, H., Cao, C.-q., and Shen, S.-z. (2018). Evolution of Primary Producers and Productivity across the Ediacaran-Cambrian Transition. *Precambrian Res.* 313, 68–77. doi:10.1016/j.precamres.2018.05.023
- Xiao, S., Bykova, N., Kovalick, A., and Gill, B. C. (2017). Stable Carbon Isotopes of Sedimentary Kerogens and Carbonaceous Macrofossils from the Ediacaran Miaohé Member in South China: Implications for Stratigraphic Correlation and Sources of Sedimentary Organic Carbon. *Precambrian Res.* 302, 171–179. doi:10.1016/j.precamres.2017.10.006

- Xiao, S., Narbonne, G. M., Zhou, C., Laflamme, M., Grazhdankin, D. V., Moczydlowska-Vidal, M., et al. (2016). Towards an Ediacaran Time Scale: Problems, Protocols, and Prospects. *Episodes* 39, 540–555. doi:10.18814/epiiugs/2016/v39i4/103886
- Xiao, S., Zhang, Y., and Knoll, A. H. (1998). Three-dimensional Preservation of Algae and Animal Embryos in a Neoproterozoic Phosphorite. *Nature* 391, 553–558. doi:10.1038/35318
- Xiao, S., Zhou, C., Liu, P., Wang, D., and Yuan, X. (2014). Phosphatized Acanthomorphic Acritarchs and Related Microfossils from the Ediacaran Doushantuo Formation at Weng'an (South China) and Their Implications for Biostratigraphic Correlation. *J. Paleontol.* 88, 1–67. doi:10.1666/12-157r
- Xu, D., Wang, X., Shi, X., Tang, D., Zhao, X., Feng, L., et al. (2020). Nitrogen Cycle Perturbations Linked to Metazoan Diversification during the Early Cambrian. *Palaeogeogr. Palaeoclimatol. Palaeoecol.* 538, 109392. doi:10.1016/j.palaeo.2019.109392
- Yin, Z., Zhu, M., Davidson, E. H., Bottjer, D. J., Zhao, F., and Tafforeau, P. (2015). Sponge Grade Body Fossil with Cellular Resolution Dating 60 Myr before the Cambrian. *Proc. Natl. Acad. Sci. USA* 112, E1453–E1460. doi:10.1073/pnas.1414577112
- Zerkle, A. L., Poulton, S. W., Newton, R. J., Mettam, C., Claire, M. W., Bekker, A., et al. (2017). Onset of the Aerobic Nitrogen Cycle during the Great Oxidation Event. *Nature* 542, 465–467. doi:10.1038/nature20826
- Zhang, F., Xiao, S., Romaniello, S. J., Hardisty, D., Li, C., Melezhik, V., et al. (2019a). Global marine Redox Changes Drove the Rise and Fall of the Ediacara Biota. *Geobiol.* 17, 594–610. doi:10.1111/gbi.12359
- Zhang, S., Jiang, G., Zhang, J., Song, B., Kennedy, M. J., and Christie-Blick, N. (2005). U-pb Sensitive High-Resolution Ion Microprobe Ages from the Doushantuo Formation in south China: Constraints on Late Neoproterozoic Glaciations. *Geol* 33, 473–476. doi:10.1130/g21418.1
- Zhang, Y., Pufahl, P. K., Du, Y., Chen, G., Liu, J., Chen, Q., et al. (2019b). Economic Phosphorite from the Ediacaran Doushantuo Formation, South China, and the Neoproterozoic-Cambrian Phosphogenic Event. *Sediment. Geol.* 388, 1–19. doi:10.1016/j.sedgeo.2019.05.004
- Zhou, C., Jiang, S., Xiao, S., Chen, Z., and Yuan, X. (2012). Rare Earth Elements and Carbon Isotope Geochemistry of the Doushantuo Formation in South China: Implication for Middle Ediacaran Shallow marine Redox Conditions. *Chin. Sci. Bull.* 57, 1998–2006. doi:10.1007/s11434-012-5082-6
- Zhou, C., and Xiao, S. (2007). Ediacaran  $\delta^{13}\text{C}$  Chemostratigraphy of South China. *Chem. Geol.* 237, 89–108. doi:10.1016/j.chemgeo.2006.06.021
- Zhou, C., Xiao, S., Wang, W., Guan, C., Ouyang, Q., and Chen, Z. (2017). The Stratigraphic Complexity of the Middle Ediacaran Carbon Isotopic Record in the Yangtze Gorges Area, South China, and its Implications for the Age and Chemostratigraphic Significance of the Shuram Excursion. *Precambrian Res.* 288, 23–38. doi:10.1016/j.precamres.2016.11.007
- Zhou, C., Yuan, X., Xiao, S., Chen, Z., and Hua, H. (2019). Ediacaran Integrative Stratigraphy and Timescale of China. *Sci. China Earth Sci.* 62, 7–24. doi:10.1007/s11430-017-9216-2
- Zhu, M., Lu, M., Zhang, J., Zhao, F., Li, G., Aihua, Y., et al. (2013). Carbon Isotope Chemostratigraphy and Sedimentary Facies Evolution of the Ediacaran Doushantuo Formation in Western Hubei, South China. *Precambrian Res.* 225, 7–28. doi:10.1016/j.precamres.2011.07.019
- Zhu, M., Zhang, J., and Yang, A. (2007). Integrated Ediacaran (Sinian) Chronostratigraphy of South China. *Palaeogeogr. Palaeoclimatol. Palaeoecol.* 254, 7–61. doi:10.1016/j.palaeo.2007.03.025

**Conflict of Interest:** The authors declare that the research was conducted in the absence of any commercial or financial relationships that could be construed as a potential conflict of interest.

Copyright © 2021 Xu, Wang, Shi, Peng and Stüeken. This is an open-access article distributed under the terms of the Creative Commons Attribution License (CC BY). The use, distribution or reproduction in other forums is permitted, provided the original author(s) and the copyright owner(s) are credited and that the original publication in this journal is cited, in accordance with accepted academic practice. No use, distribution or reproduction is permitted which does not comply with these terms.